Short title: ONAC127 and ONAC129 regulate rice grain filling

A Heat Stress Responsive NAC Transcription Factor Heterodimer Plays Key Roles in Rice Caryopsis Filling

Ye Ren, Zhouquan Huang, Hao Jiang, Zhuo Wang, Fengsheng Wu, Yufei Xiong, Jialing Yao *

College of Life Science and Technology, Huazhong Agricultural University, Wuhan 430070, China.

Corresponding author: Jialing Yao, Ph.D. and Professor, College of Life Science and Technology, Huazhong Agricultural University, Wuhan 430070, China.

* Address correspondence to yaojlmy@mail.hzau.edu.cn

Telephone: 86-27-87282866

Fax: 86-27-87282866

ABSTRACT

High temperature usually leads to the failure of grain filling during caryopsis development, resulting in the loss of yield, however the mechanism is not yet well elucidated. Here, we report that two rice caryopsis-specific NAM/ATAF/CUC domain transcription factors, *ONAC127* and *ONAC129*, respond to heat stress and are involved in the caryopsis filling process. *ONAC127* and *ONAC129* are dominantly expressed in pericarp during grain filling and can form a heterodimer. To investigate the functions of these two ONACs, we obtained CRISPR/cas9 induced mutants and overexpression lines of them. Interestingly, we found that both knock-out and overexpression plants showed incompletely filling and shrunken phenotype of caryopses, which became more severe under heat stress. The shrunken caryopses of these transgenic lines are usually with ectopic accumulation of starch in the pericarp. Transcriptome analyses revealed that *ONAC127* and *ONAC129* mainly regulate stimulus response, cell wall construction and nutrient transport etc. ChIP-seq analyses identified the direct targets of ONAC127 and ONAC129 in developing caryopses, including monosaccharide transporter *OsMST6*, sugar transporter *OsSWEET4*, calmodulin-like protein *OsMSR2* and Ethylene-Response AP2/ERF Factor *OsEATB*. The result suggested that *ONAC127* and *ONAC129* might regulate the caryopsis filling through sugar transportation and abiotic stress responses. Overall, this study demonstrates the transcriptional regulatory networks involving ONAC127 and ONAC129, which coordinates multiple pathways to modulate caryopsis development and heat stress response at rice filling stage.

INTRODUCTION

Rice caryopsis development starts from the fertilized ovary and finishes with a dehydrated, hard and transparent grain. This process can be divided into three stages by landmark events: cell division, organogenesis and maturation. (Agarwal et al., 2011). A rice caryopsis is mainly composed of endosperm filled with starch grains, and the biosynthesis of starch is closely related to carbohydrates transportation. Carbohydrates are synthesized in leaves and delivered to caryopses via phloem (Patrick, 1997), then unloaded to the pericarp as the energy and materials for starch biosynthesis (Zhang et al., 2007). The dorsal vascular bundle passes through the pericarp is the main nutrient transport tissue in caryopsis (Oparka and Gates, 1981). While the vascular bundles are not contiguous with endosperm tissue (Hoshikawa, 1984), the apoplasmic pathway is the only way for nutrient to reach the starchy endosperm. (Matsuda et al., 1979).

Carbohydrates may enter the nucellar epidermis directly through plasmodesmata, then be transported to the apoplasmic space with sugar transporter protein OsSWEETs (sugar will eventually be exported transporters) and partially hydrolyzed into monosaccharide by cell wall invertase OsCINs. The monosaccharide is transported into the aleurone layer mainly by monosaccharide transporter OsMSTs while the rest un-hydrolyzed sucrose is directly transported into the aleurone layer via sucrose transporter OsSUTs (Yang et al., 2018). The nutrient transportation is also regulated by a range of transcription factors such as *OsNF-YB1* and *OsNF-YC12*, which activate the expression of OsSUTs to capture the leaked sucrose in apoplasmic space. Knockout of *NF-YB1* or *OsNF-YC12* leads to defective grains with chalky endosperms and similar phenotype has been observed in mutants of *OsSUT1* (Bai et al., 2016; Xiong et al., 2019).

The nutrient transport processes in caryopsis are susceptible to changing environmental conditions, extreme external stimuli (especially the extreme temperature) during grain-filling stage will lead to a reduction of nearly 50% in rice (Hu and Xiong, 2014). Plants respond to the unexpected high temperature through some stress-specific signaling pathways. During heat stress signal transduction, the heat shock transcription

72 factors (HSFs) will be activated to regulate the expression of downstream heat shock
73 proteins (HSPs) and other stress-related genes. For example, AP2/EREBP transcription
74 factor *DREB2A* can activate a heat shock transcription factor *hsfA3* under heat stress to
75 induce the expression of specific HSPs (Schramm et al., 2008). Similarly, the
76 expression of *OsbZIP60*, which play important roles in moisture retention and heat-
77 damage resistance, is induced under heat stress and endoplasmic reticulum stress (Oono
78 et al., 2010). Although several plant heat stress response related proteins have been
79 found and elucidated, the mechanisms of the response are still poorly understood.
80 NAC (NAM, ATAF1/2, CUC2) transcription factors are one of the largest family
81 of plant specific transcription factors with 151 members in rice (Nuruzzaman et al.,
82 2010). The typical structure of NAC transcription factors is a conserved NAC domain
83 with about 150 amino acids in N-terminus, followed by a variable transcriptional
84 regulation region (TRR) in C-terminus (Christianson et al., 2010). The NAC domain
85 can be further subdivided into five subdomains [A-E], subdomains C and D are highly
86 conserved and may mainly act in DNA-binding (Ooka et al., 2003). In addition, some
87 subdomain D contains a hydrophobic NAC repression domain (NARD) which can
88 suppress the transcriptional activity of NAC transcription factors by suppressing their
89 DNA-binding ability or nuclear localization ability. The specific functional motif in
90 NARD, LVFY can suppress not only the activity of NAC transcription factors, but also
91 the other transcription factors by its hydrophobicity (Hao et al., 2010).
92 NAC transcription factors are involved in many biological processes in plants, such
93 as organ development, secondary wall synthesis, stress response and so on. For instance,
94 *NAC29* and *NAC31* regulate downstream cellulose synthase (CESA) by activating the
95 downstream transcription factor *MYB61* to control the synthesis of secondary wall
96 (Huang et al., 2015). For stress response, especially in abiotic ways, the NAC
97 transcription factors are master regulators in this process. *RD26* gene is the first NAC
98 transcription factor identified as a regulator in mediating abscisic acid (ABA) and
99 jasmonate (JA) signaling during stress responses in Arabidopsis (Fujita et al., 2004).

SNAC1 is a stress-responsive NAC transcription factor confers rice drought tolerance by closing stomata (Hu et al., 2006) and *SNAC3* confers heat and drought tolerance through regulation of reactive oxygen species (Fang et al., 2015). *OsNAC2* is also reported involving in drought stress response mediated by ABA (Shen et al., 2017). Meanwhile, it plays divergent roles in different biological processes, such as regulating shoot branching (Mao et al., 2007), affecting plant height and flowering time through mediating the gibberellic acid (GA) pathway (Chen et al., 2015). *VNI2* in Arabidopsis is a bifunctional NAC transcription factor reported as a transcriptional repressor functioning in xylem vessel formation (Yamaguchi et al., 2010), but the transcriptional activator activity of *VNI2* is induced by high salinity stress to regulate the leaf longevity (Yang et al., 2011).

Nine caryopsis-specific NAC transcription factors were found through transcriptome analyses in rice (Mathew et al., 2016).We selected four of these genes, *ONAC025*, *ONAC127*, *ONAC128* and *ONAC129* for further analyses, which located in the linked regions of chromosome 11 and were identified as a gene cluster (Fang et al., 2008). As recent study implied two NAC transcription factors specifically expressed in maize seeds, *ZmNAC128* and *ZmNAC130*, playing critical roles in starch and protein accumulation in seeds filling (Zhang et al., 2019). We inferred that the four NAC transcriptional factors might also be involved in some important processes in rice caryopsis development. In this study, we selected *ONAC127* and *ONAC129* from the four genes, which could form a heterodimer and participate in apoplasmic transportation as well as heat stress response to regulate rice caryopsis filling. These findings broadened the understanding of the regulation network of stress response and grain filling in rice.

RESULTS

ONAC127 and *ONAC129* are specifically expressed in caryopsis

To understand these four genes basically, we firstly checked the expression data of

ONAC025, *ONAC127*, *ONAC128* and *ONAC129* in the microarray database CREP (http://crep.ncpgr.cn) (Wang et al., 2010). The data showed that the expression level of *ONAC025* in caryopsis was significantly higher than that of the rest genes, while that of *ONAC128* was the lowest among the four genes. For *ONAC127* and *ONAC129*, they showed the highest expression level at 7 d after pollination (DAP) and then decreased gradually, such similar expression pattern attracted our further attention.

For validating the spatial and temporal expression patterns and further exploring the specific expression distribution of *ONAC127* and *ONAC129* in caryopsis, we mechanically isolated rice caryopses at 5-14 DAP to the mixture of pericarp and aleurone layer, starch endosperm and embryo for qRT-PCR analyses by the method described by Bai (Bai et al., 2016). The aleurone layer specifically expressed gene *oleosin* and the starch endosperm specifically expressed gene *SDBE* were used as markers (Ishimaru et al., 2015) (Supplemental Fig. S1). The result showed that *ONAC127* and *ONAC129* were mainly expressed in pericarp or aleurone layer while they were weakly expressed in starch endosperm, and the expression went to the summit at 5 DAP during the whole development process (Fig. 1A).

The mRNA *in situ* hybridization analyses using the unripe caryopses of ZH11 turned out that *ONAC127* and *ONAC129* were dominantly expressed in pericarp, when the expression level in aleurone layer and starch endosperm were quite weak (Fig. 1B). Histochemical GUS activity was also detected using the transgenic plants expressing pONAC127::GUS and pONAC129::GUS, the result was almost identical to that of *in situ* hybridization analyses, that *ONAC127* and *ONAC129* were preferentially expressed in pericarp of caryopsis (Fig. 1C). Considering that 5 DAP is a key time point of caryopsis development for the organogenesis is finished and maturation stage is just initiated (Agarwal et al., 2011). *ONAC127* and *ONAC129* might be involved in some substance exchange processes playing vital roles in caryopsis filling and maturation.

We then carried out the assay through transforming green fluorescent protein (GFP) fused ONAC127 or ONAC129 protein into rice protoplast transiently to investigate the

subcellular localization pattern of the two genes. 35S::GFP was used as a positive control and 35S::Ghd7-CFP was used as a nuclear marker (Xue et al., 2008). The fluorescence generated by ONAC127-GFP and ONAC129-GFP was distributed in the nucleus and cytoplasm just like the way positive control did (Fig. 1D). For further confirming the subcellular localization, transgenic plants expressing pUbi::ONAC127-GFP and pUbi::ONAC129-GFP were generated in Zhonghua11 (ZH11) background. The subcellular localization pattern of ONAC127 and ONAC129 were validated by detecting the fluorescence from the roots of two-week-old rice seedlings of the plants, ONAC127 and ONAC129 proteins were indeed localized in the nucleus and cytoplasm (Supplemental Fig. S2).

ONAC127 and ONAC129 can form a heterodimer

It was noticed that the NAC transcription factors usually function as a dimer (Olsen et al., 2005), thus we investigated if there was any interaction between ONAC127 and ONAC129. The result indicated that ONAC127 could interact with ONAC129 in yeast (Fig. 2A). To confirm the interaction between ONAC127 and ONAC129, the *in vitro* GST pull-down assay was carried out. His-tagged ONAC127 and GST-tagged ONAC129 were expressed respectively and incubated together. The protein mixture of GST and ONAC127-His was used as a negative control. After purification by Glutathione Agarose, ONAC127-His was detected in the sample containing ONAC129-GST instead of the control with His-tag antibody (Fig. 2B). The *in vivo* bimolecular fluorescence complementation (BiFC) assay was also performed with rice protoplasts. Nuclear homodimer OsbZIP63 was chosen as positive control (Walter et al., 2004), and 35S::Ghd7-CFP was used as a nuclear marker. Yellow fluorescence generated from the interaction between ONAC127-YFP^N and ONAC129-YFP^C was detected, which confirmed the heterodimer ONAC127 and ONAC129 formed in nucleus (Fig. 2C). In view of previous studies, some of NAC transcription factors were located in the cytoplasm or plasma membrane first, and then were imported to nuclei

under some specific conditions (Fang et al., 2014). Considering the subcellular localization pattern of ONAC127 and ONAC129 (Fig. 1D), we speculated that these two proteins might also exert their transcriptional regulation functions in this way.

ONAC127 **and** ***ONAC129*** **are key players in starch accumulation during rice caryopsis filling**

We obtained the specifically knockout *ONAC127* or *ONAC129* mutants (*onac127* and *onac129*) in ZH11 background by CRISPR/Cas9 genome editing system (Ma et al., 2015). Considering that these two proteins could form a heterodimer, double knockout mutants (*onac127;129*) were also obtained. The sgRNA target sites were designed at the exons of *ONAC127* and *ONAC129* using the web-based tool CRISPR-P (Liu et al., 2017). There are two target sites of each gene, which were expected to generate different mutations in the coding region of the genes (Fig. 3A). The grains of three T_0 homozygous plants of each mutant were selected for generating independent T_1 transgenic lines. The sequencing data of the transgenic lines was decoded by the method described by Liu (Liu et al., 2015), and the genotypes of the homozygous lines were showed in Supplemental Fig. S3. On the other hand, we also generated the overexpression lines pUbi::ONAC127-FLAG and pUbi::ONAC129-FLAG (OX127 and OX129) (Fig. 3B). Relative expression level of the overexpression lines was analyzed by qRT-PCR (Supplemental Fig. S4).

During the rice reproductive stage, we found the development of caryopses in *ONAC127* and *ONAC129* transgenic lines arrested during 5-7 DAP (Supplemental Fig. S5), resulting in shrunken and incompletely filled grains after ripening (Fig. 3C, D). As we mentioned before, the expression level of *ONAC127* and *ONAC129* was very high during 5-7 DAP (Fig. 1A), the functions of *ONAC127* and *ONAC129* seem to be closely related to grain filling, especially at the early stage of maturation. Since the phenotype is illogical, we detected the expression level of the two ONACs in the transgenic lines immediately. It turned out that the expression of *ONAC127* and *ONAC129* was up-

209 regulated in the overexpression lines and down-regulated in the mutants indeed
210 (Supplemental Fig. S6). We speculated that ONAC127 and ONAC129 may regulate
211 several different pathways contributing to caryopsis filling at the same time. The
212 expression of the two ONACs may need to be maintained at a steady level, any
213 fluctuations in their expression would interfere the normal running of different
214 pathways and have the chance to bring caryopsis filling defection.

215 To investigate the reason of the shrunken phenotype further, histological analyses
216 through resin embedded sections were prepared with 7 DAP incompletely filling
217 caryopses. In ZH11, starch was stored transiently in the pericarp during the early stage,
218 the degradation of starch in the pericarp correlated with starch accumulation in the
219 endosperm (Wu et al., 2016). As we expected, the starch in the endosperm of ZH11
220 caryopses was arrayed neatly, densely and hardly found in pericarp (Fig. 3E). In
221 contrast, many starch grains accumulated in the pericarp of the mutants and the
222 overexpression lines of *ONAC127* and *ONAC129*, especially in the double mutant
223 *onac127;129*, in which substantial starch grains were hardly seen in endosperm (Fig.
224 3E). The finding above suggested that *ONAC127* and *ONAC129* might play critical
225 roles in starch translocation and mobilization towards the developing endosperm.

226 **ONAC127 and ONAC129 are involved in heat stress response**

227 With the measurement of agronomic traits, the transgenic lines of *ONAC127* and
228 *ONAC129* showed significant reduction in both seed set rate (percentage of fully filled
229 seeds after harvest) and 1000-grains weight (Fig. 4A, B). The percentage of shrunken
230 grains showed an obvious increase while proportion of blighted grains (glumes with no
231 seed in it) did not change significantly in these transgenic lines (Fig. 4C). It proved that
232 the reduction of seed set rate and yield was mainly caused by the increase of shrunken
233 grains.

234 Notably, the transgenic plants during filling stages were suffered from severe heat
235 stress in the summer of 2018 (Fig. 4D, E). Previous studies have shown that the ambient

236 temperature higher than 35℃ would have a serious impact on the yield at flowering
237 and grain filling stages (Hakata et al., 2017). Therefore, we set 35℃ as the heat damage
238 temperature of rice (T_B), and calculated the heat damage accumulated temperature per
239 hour (TH_i), heat damage accumulated temperature during filling stage (T_S) and heat
240 damage hours during filling stage (H_S) as described by Chen (Chen et al., 2019). Given
241 that *ONAC127* and *ONAC129* function during early filling stage, we also calculated the
242 heat damage accumulated temperature during 0-7 DAP (T_{S7}) and heat damage hours
243 during 0-7 DAP (H_{S7}). Noting that we cultivated two batches of rice in the summer of
244 2018, the first batch of plants were flowering on about July 20 when the second batch
245 goes on about August 20. It's obvious that T_S and H_S of the first batch were much higher
246 than that of the second batch, especially at the early development stage of caryopsis
247 (Fig. 4D, E).Therefore, the caryopses of the plants cultivated in the first batch were
248 defined as suffering from heat stress while those in the second batch were defined as
249 planted under normal conditions with little or no heat stress. We found that heat stress
250 caused sharp increase of shrunken grains compared to normal conditions, and such
251 increase in *onac127;129* was more dramatic than the other transgenic lines (Fig. 4C),
252 which led to significant decrease of seed set rate and 1000-grains weight (Fig. 4A, B).
253 Meanwhile, the expression level of *ONAC127* and *ONAC129* was highly increased
254 under heat stress (Supplemental Fig. S6), which suggested that *ONAC127* and
255 *ONAC129* might be involved in heat stress response during caryopsis filling stage.

256 **ONAC129 negatively regulates ONAC127 transcriptional activity**

257 For deeper exploring the relationship of *ONAC127* and *ONAC129*, we performed
258 a dual luciferase assay in rice protoplasts as the transcriptional activity of the two genes
259 was not detected in yeast assays (Fig. 2A). *ONAC127* and *ONAC129* were fused with
260 the yeast GAL4 binding domain (GAL4BD) as effectors to be co-transformed into rice
261 protoplasts with a firefly luciferase reporter gene driven by a CaMV35S promotor (35S-
262 GAL4-fLUC; Fig. 5A). A significant increase in the transcriptional activation activity

of ONAC127 and ONAC129 was detected, while the transcriptional activity of ONAC127 was significantly restrained when ONAC129 was co-transformed into rice protoplasts (Fig. 5B). These results hinted that ONAC129 might regulate the transcriptional activity of ONAC127 negatively and we wonder if ONAC129 could regulate the expression of *ONAC127*. However, we didn't find significant fluctuation of the expression of *ONAC127* in the transgenic lines of *ONAC129* and vice versa. (Supplemental Fig. S6).

As we know, several NAC transcription factors contain both transcriptional activation domain and NAC repression domain (NARD), which means that the combinatorial effects of both transcriptional regulation activities determine downstream events (Hao et al., 2010). Hence, we decided to BLAST and analyze the protein sequences of ONAC127 and ONAC129 through the method described by Hao, and we found that there were NARD-like sequences in NAC subdomain D indeed in both genes (Fig. 5C), which suggested that *ONAC127* and *ONAC129* might be bifunctional transcription factors that could activate or repress downstream genes in different situation.

ONAC127 and ONAC129 regulate the transcription of genes related to sugar transportation and abiotic stimulus

RNA-Seq analyses worked in identifying differentially expressed genes. The 7 DAP caryopses of the overexpression lines and mutants of *ONAC127* and *ONAC129* under heat stress and normal conditions were used to generate RNA-seq libraries. There are 7056, 6485, 5765, and 1608 differentially expressed genes (DEGHs) identified in *onac127* (*onac127*H), *onac129* (*onac129*H), OX127 (OX127H), OX129 (OX129H) respectively under heat stress, compared with ZH11 (ZH11H), and 15334, 13284, 1776, 2041 differentially expressed genes (DEGNs) which were identified in *onac127* (*onac127*N), *onac129* (*onac129*N), OX127 (OX127N), OX129 (OX129N) respectively under normal conditions compared with ZH11 (ZH11N) (Fig. 6A, B; Supplemental

Dataset S1). Gene Ontology (GO) enrichment analyses was performed to examine the biological roles of DEGs in caryopsis development. The significantly enriched GO terms were mainly associated with stimulus response, transcriptional activity regulation, signal transduction, cell wall construction and substance transportation (Fig. 6C).

Subsequently, the genes directly bound by ONAC127 and ONAC129 in caryopsis were identified using Chromatin Immunoprecipitation Sequencing assays (ChIP-seq). The ChIP assays were performed using the anti-FLAG antibody with 7 DAP caryopses of OX127 (OX127H), OX129 (OX129H) under heat stress, and OX127 (OX127N), OX129 (OX129N) under normal condition. The expression of the ONAC127-FLAG and ONAC129-FLAG fusion proteins was verified by western blot analyses to validate the effectiveness of the FLAG tags (Supplemental Fig. S7). After sequencing, 185, 6125, 220, 455 peaks were finally obtained respectively in OX127H, OX127N, OX129H and OX129N (Supplemental Dataset S2), and 54, 5092, 82, 212 putative ONAC127 and ONAC129 bound genes were identified in OX127H, OX127N, OX129H and OX129N respectively among the peaks (Fig. 6D). Then, we identified the binding motifs of the ONACs using MEME (Machanick and Bailey, 2011), and found that the significantly enriched motif was 'CT(C)TTCT(C)TT' (Fig. 6E, F), in line with 'TT(A/C/G)CTT', the specific motif of transmembrane NAC transcription factors *NTL6* and *NTL8* (Lindemose et al., 2014). Both the two genes were associated with stimulus response, implying that *ONAC127* and *ONAC129* were probably involved in stress response. Notably, the motif 'CT(C)TTCT(C)TT' was only found significantly in OX127H and OX129H. There was no significantly enriched motif in OX127N and OX129N, implying that the target genes of ONAC127 and ONAC129 might be more specific under heat stress.

For further exploring the target genes regulated by ONAC127 and ONAC129, we defined the genes which were either consistently bound by ONAC127/129 or simultaneously bound by ONAC127 and ONAC129 under heat stress or normal conditions as ONAC127/129 preferable-bound genes (Fig. 6D, red trapezoid). Based

on the data from RNA-Seq analyses and phenotype of transgenic lines of ONAC127 and ONAC129, 8 genes with respect to sugar transportation or abiotic stress response were selected from 136 preferable-bound genes as the potential target genes (PTGs) of ONAC127 and ONAC129 for further investigation.

ONAC127 and ONAC129 play a pivotal role in caryopsis filling through regulating key factors directly in substance accumulation and stress response

To validate the interactions between ONAC127/129 and promotors of their potential target genes (PTGs), the yeast one-hybrid assays were performed. It suggested that ONAC127 and ONAC129 could bind to the promoter sequences of *OsEATB*, *OsHCI1*, *OsMSR2*, *OsSWEET4*, *bHLH144* and *OsMST6* directly in yeast (Fig. 7A). The Dual-LUC assays in rice protoplasts were performed to figure out whether ONAC127 and ONAC129 affect the transcription of these genes directly. ONAC127 and ONAC129 were co-transformed into rice protoplasts with a firefly luciferase reporter gene driven by target gene promotors (Fig. 7B). It turned out that ONAC127 activated *OsMSR2* and *OsMST6* promotors significantly, and both ONAC127 and ONAC129 repressed the *OsEATB* and *OsSWEET4* promotors strongly *in vivo*. It is noteworthy that ONAC129 could suppress the transcriptional activation activity of ONAC127 to *OsMSR2* and *OsMST6* promotors, while ONAC129 barely regulated the transcription of *OsMSR2* and *OsMST6* alone (Fig. 7C).

For testing whether the endogenous ONAC127 and ONAC129 bound to the target genes specifically, ChIP-qPCR was performed using the same rice materials of ChIP-Seq. The result indicated that ONAC127 and ONAC129 bound to the promoters of *OsEATB*, *OsMSR2*, *OsSWEET4* and *OsMST6* respectively under heat stress and normal conditions (Fig. 7D, E, F, G). The qRT-PCR for these genes was also performed in the 7 DAP caryopses of transgenic lines of *ONAC127* and *ONAC129*, showing that the expression of *OsEATB* and *OsSWEET4* was significantly up-regulated in the mutants and generally down-regulated in the overexpression lines. The expression of *OsMSR2*

and *OsMST6* was both up-regulated in *onac129* and down-regulated in *onac127* (Supplemental Fig. S8). The results above indicated that *OsEATB*, *OsMSR2*, *OsSWEET4* and *OsMST6* were the direct targets of ONAC127 and ONAC129 in rice during caryopsis filling.

DISCUSSION

In this study, two rice caryopsis-specific NAC transcription factors *ONAC127* and *ONAC129* were identified, which can form a heterodimer and are predominantly expressed during the early and middle stage of rice caryopsis development (Fig. 1, 2). The caryopses of the transgenic plants were obviously unfilled (Fig. 3C, D, E; Supplemental Fig. S5), and the proportion of shrunken grains was higher under natural heat stress (Fig. 4C). By protein−DNA binding assays, we found that ONAC127 and ONAC129 may regulate the expression of the sugar transporters, *OsMST6* and *OsSWEET4* directly. Both the two genes are involved in the transportation of photosynthate from dorsal vascular bundles to endosperm during caryopsis filling (Wang et al., 2008; Sosso et al., 2015). ONAC127 and ONAC129 also bind to the promotors of *OsMSR2* and *OsEATB* directly (Fig. 7), which participate in abiotic stress responses by responding to calcium ion (Ca^{2+}) or plant hormones (Qi et al., 2011; Xu et al., 2011). These findings suggest that *ONAC127* and *ONAC129* may be involved in multiple pathways, therefore interfere the abiotic stress response and caryopsis filling process during rice reproductive stage.

ONAC127 and ONAC129 are involved in the apoplasmic transportation of photosynthates as a balancer

At the early stage of caryopsis development, some of the photosynthate from the dorsal vascular bundle was transported to endosperm through the apoplasmic space formed by degenerative nucellar cell wall, the others synthesized the starch grains in mesocarp cells (Hoshikawa, 1984). The starch accumulation in pericarp will reach a

maximum at 5 DAP. After that, the starch in mesocarp cells will be disintegrated and the nutrient will be transported to the endosperm due to the continuous process of endosperm cells filling. The cell contents of pericarp cells will disappear, and the cells will eventually dehydrate and die, leaving only the cuticularized cell wall remnants (Wu et al., 2016).

Since the abnormal expression of *ONAC127* and *ONAC129*, endosperm cells in abnormal caryopses may not obtain enough photosynthate for filling due to the functional defect of apoplasmic transport pathways. The photosynthates accumulates in pericarp as starch grains without been disintegrated, thus stop the endosperm cells from proliferation or filling by starch, eventually leading to incompletely filled and shrunken caryopsis (Fig. 3C, E).

It is noteworthy that the target transporters *OsSWEET4* and *OsMST6* are predominantly expressed at early stages of caryopsis development, and may act in downstream of the cell wall invertase OsCIN2 to import hexose into aleurone layer through apoplasmic space (Wang et al., 2008; Sosso et al., 2015; Yang et al., 2018). As previously mentioned, ONAC127 and ONAC129 suppress the expression of *OsSWEET4* directly (Fig. 7C; Supplemental Fig. S8), and *ossweet4-1*, the mutant of *OsSWEET4*, has a distinct phenotype with shrunken grains similar with the abnormal caryopses in transgenic lines of *ONAC127* and *ONAC129* (Sosso et al., 2015). The fact confirmed our hypothesis that *ONAC127* and *ONAC129* are involved in the apoplasmic transport pathways directly by regulating the expression of transporters indeed.

Moreover, the shrunken caryopses we observed in mutants and overexpression lines of *ONAC127* and *ONAC129* are also similar with the incompletely filled caryopses of the double mutants *ossweet11;15*, in which two apoplasmic transporters OsSWEET11 and OsSWEET15 were dysfunction (Yang et al., 2018). For that *OsSWEET15* has been excluded from the target genes by the yeast one-hybrid assays (Fig. 7A), we detected the expression of *OsSWEET11* and *OsSWEET15* in transgenic lines of *ONAC127* and *ONAC129* by qRT-PCR and found that both genes might be

399 activated by ONAC127 and ONAC129 indirectly (Supplemental Fig. S9). The fact
400 suggested that ONAC127 and ONAC129 might activate the expression of
401 *OsSWEET11/15* and suppress the expression of *OsSWEET4* simultaneously. This may
402 explain the fact that the phenotypes of mutants and overexpression lines of *ONAC127*
403 and *ONAC129* are almost the same in incompletely filled caryopses (Fig. 3C, D, E;
404 Supplemental Fig. S5). Hence, we speculate that *ONAC127* and *ONAC129* may act as
405 a balancer in apoplasmic transportation by activating or suppressing the expression of
406 transporters dynamically (Fig. 8), therefore keeping the amount of several different
407 apoplasmic transporters at different stages of caryopsis development.
408 ONAC129 suppresses the transcriptional activity of ONAC127 in some pathways,
409 meanwhile, ONAC127 and ONAC129 may regulate downstream genes differently at
410 dimer state and monomer state (Fig. 5B, 7C). We conjecture that the proportion of
411 ONAC127/129 dimers may be vital in adjusting the balance of the amount of
412 apoplasmic transporters at different stages of caryopsis development. Whether to
413 knockout or to over-express *ONAC127* or *ONAC129*, the proportion of the monomers
414 and dimers of ONAC127/129 will be changed inevitably, which induces various
415 changes in expression of the apoplasmic transporters, thus the apoplasmic
416 transportation defects, leading to the incomplete filling caryopsis phenotype (Fig. 3C).
417 In macroscopic view, the balance regulation of apoplasmic transportation may be a
418 "rate-limiting step" of rice reproductive growth to ensure that the photosynthate is
419 enough for both the filling of grains and the energy for plants to avoid premature aging,
420 thus may be vital for plants to keep the balance of vegetative growth and reproductive
421 growth.

422 **ONAC127 and ONAC129 respond to heat stress during caryopsis filling**

423 Heat stress has profound effects on plant growth, particularly in reproductive
424 development. When plants encounter heat stress, the rise of cytosolic Ca^{2+}
425 concentration is the most rapid response (Liu et al., 2003). With the increase of Ca^{2+}

426 concentration, the expression of calmodulins (CaMs) and Calmodulin-like genes
427 (CMLs) will be activated and modulate the phosphorylation state of HSFs to regulate
428 their DNA binding ability, thereby regulating the expression of heat stress related genes
429 including HSPs and some plant hormone responsive genes (Li et al., 2018).

430 The proportion of incompletely filled caryopses under heat stress is much higher
431 than that of normal condition (Fig. 4C), and the expression of *ONAC127* and *ONAC129*
432 was induced by heat stress (Supplemental Fig. S6), suggesting that heat stress might
433 interfere the dimerization of ONAC127 and ONAC129 to affect the balance of
434 apoplastic transportation. As previously mentioned, ONAC127 and ONAC129 regulate
435 the expression of *OsMSR2* and *OsEATB* directly (Fig. 6C; Supplemental Fig. S8).
436 Previous study showed that *OsMSR2*, which can be strongly induced by heat, cold and
437 drought stress, is a calmodulin-like protein working by binding Ca^{2+} and speculated
438 having the function as a Ca^{2+} sensor in plant cells (Xu et al., 2011). *OsEATB* is a rice
439 AP2/ERF gene which can suppress gibberellic acid (GA) synthesis while the GA
440 signaling pathway involved in the regulation of cell elongation and morphogenesis
441 under heat stress (Koini et al., 2009; Qi et al., 2011). We hereby speculated that
442 *ONAC127* and *ONAC129* might participate in heat stress response by regulating the
443 Ca^{2+} and GA signaling pathway.

444 The expression level of *OsHSP101* and *OsHCI1* was changed significantly in the
445 transgenic lines of *ONAC127* and *ONAC129* (Fig. 7A, C; Supplemental Fig. S9). We
446 believe that they are also the potential target genes of ONAC127 and ONAC129, though
447 they may not be regulated directly. RING E3 ligase gene *OsHCI1* is induced by heat
448 stress and mediates nuclear–cytoplasmic trafficking of nuclear substrate proteins via
449 mono-ubiquitination to improve the heat tolerance under heat shock (Lim et al., 2013).
450 Meanwhile, OsHSP101 function as one of the important molecular chaperones that
451 interact with OsHSA32 and OsHsfA2c, the latter of which is one of the central
452 regulators of heat stress response (Singh et al., 2012; Lin et al., 2014). Accordingly, we
453 believe that *ONAC127* and *ONAC129* are involved in some core reactions in the heat

454 stress response during rice caryopsis development stage.

455 Ca^{2+} is one of the most important second messengers in heat stress response,
456 cytosolic Ca^{2+} concentration would change rapidly in a short time when heat stress
457 occurs (Li et al., 2018). The stress signal would be then transmitted by CaMs/CMLs
458 like OsMSR2 to influence downstream gene expression consequently. When the
459 downstream HSFs are activated, HSPs including OsHSP101 would be induced to
460 express and function, and some nuclear-cytoplasmic trafficking reactions involving
461 OsHCI1 would occur (Singh et al., 2012; Lim et al., 2013). Besides, a variety of plant
462 hormones including GA would act in heat stress response to maintain plant growth, and
463 *OsEATB* plays an important role in GA-mediated plant cell elongation (Qi et al., 2011;
464 Li et al., 2018). Considering that all these direct or indirect target genes of *ONAC127*
465 and *ONAC129* play vital roles in the key steps of the heat stress response regulatory
466 network, we speculate that ONAC127 and ONAC129 may be the core transcription
467 factors in heat stress response during rice caryopsis filling stage, and the stress and
468 hormone response may be involved in the complex regulatory network of apoplasmic
469 transportation.

470 **MATERIALS AND METHODS**

471 **Generation of transgenic plants and growth conditions**

472 For generating CRISPR mutants, we used the web-based tool CRISPR-P v2.0
473 (http://cbi.hzau.edu.cn/CRISPR2/) designed by Liu (Liu et al., 2017) to get the specific
474 gRNA cassettes targeting *ONAC127* and *ONAC129* and then cloned into a binary vector
475 pYLCRISPR/Cas9-MH (Ma et al., 2015). For overexpression plants, we amplified the
476 stop-code-less cDNA fragments of *ONAC127* and *ONAC129*, fused 3×Flag or EGFP
477 coding sequence at the 3' end. The fused sequences were cloned into the binary vector
478 pCAMBIA1301U (driven by a maize ubiquitin promotor). For tissue specific
479 expression analyses, a 2000bp fragment of the 5' upstream region of *ONAC127*, and a
480 2043bp fragment of the 5' upstream region of *ONAC129* were cloned into the binary

vector pDX2181G (with GUS, β-glucuronidase).These recombinant constructs were introduced into rice Zhonghua11 (ZH11; *Oryza sativa* ssp. *japonica)* by *Agrobacterium tumefaciens* (EH105)-mediated transformation (Lin and Zhang, 2005). The plant materials were cultivated in paddy fields in Huazhong Agricultural University, Wuhan, China, under natural long-day conditions (approximately 12-14 h light/10-12 h dark) during May to October 2018. The temperature of growing areas during rice reproductive stage was showed in (Fig. 4D, E). We set 35℃ as the heat damage temperature of rice (T_B), and calculated the heat damage accumulated temperature per hour (TH_i), $TH_i = \begin{cases} T_i - T_B & T_i \geq T_B \\ 0 & T_i < T_B \end{cases}$ (T_i is the ambient temperature at *i* hour); heat damage hours during filling stage (H_S) , $H_s = \sum_{i=0}^{n} H_i$ $(H_i = \begin{cases} 1 & T_i \geq T_B \\ 0 & T_i < T_B \end{cases})$ and heat damage accumulated temperature during filling stage (T_S), $T_S = \sum_{i=0}^{n} TH_i$ using the method described by Chen (Chen et al., 2019). The heat damage accumulated temperature during 0-7 DAP (T_{S7}) and heat damage hours during 0-7 DAP (H_{S7}) was also calculated as the method above. The phenotypes were detected in homozygous T_1 generation of transgenic plants. The primer sequences used in this study were listed in Supplemental Table S1 and would not be repeated in the following article.

Histochemical GUS staining

Unripe caryopses at 5 and 7 DAP from pONAC127::GUS and pONAC129::GUS transgenic plants were collected for the GUS staining assays following the methods described by Yang (Yang et al., 2018).

Microscopy analyses

For semithin section microscopy analyses, the unripe caryopses at 7 DAP were collected in 2.5% glutaraldehyde for fixation, vacuum infiltrated on ice for 30 min and incubated at 4℃ for 24h. The plastic embedding and sectioning were performed as described by Wang (Wang et al., 2008). Slides were stained with toluidine blue and

506 detected by a BX53 microscope (Olympus).

507 **RNA *in situ* hybridization**

508 Unripe caryopses (1-10 DAP) from rice ZH11 were collected for paraffin
509 embedding. Paraffin section was performed according to the previous method (Xiong
510 et al., 2019). Gene-specific fragments of *ONAC127* and *ONAC129* were amplified by
511 the primers used in RT-PCR and cloned into the pGM-T vector. The probes were
512 synthesized using the DIG RNA labeling kit (SP6/T7) (Roche) according to the
513 manufacturer's recommendations. RNA hybridization and immunologic detection of
514 the hybridized probes were performed on sections as described by Kouchi (Kouchi and
515 Hata, 1993). Slides were observed using a BX53 microscope (Olympus).

516 **Transient expression assays**

517 To investigate the subcellular localization of ONAC127 and ONAC129, the CDS
518 of these genes were cloned into the pM999-35S vector, the nuclear located gene *Ghd7*
519 was used as a nuclear localization marker (Xue et al., 2008).For the BiFC assays, the
520 CDS of *ONAC127* and *ONAC129* were cloned into the vectors pVYNE and pVYCE
521 (Waadt et al., 2008) respectively. Plasmids were extracted and purified using the
522 Plasmid Midi Kit (QIAGEN) and were then transformed into rice protoplasts according
523 to the procedure described by Shen (Shen et al., 2017). The fluorescent signals were
524 detected with a confocal laser scanning microscope (TCS SP8, Leica).

525 **RNA isolation and transcript analyses**

526 Total RNA was isolated using the TRIzol method (Invitrogen), and the first strand
527 cDNA was synthesized using HiScript II Reverse Transcriptase (Vazyme). The real-
528 time PCR was performed on QuantStudio 7 Flex Real-Time PCR System (Applied
529 Biosystems), with the $2^{-\Delta\Delta Ct}$ method for relative quantification (Livak and Schmittgen,
530 2001). The significance of differences was estimated using Student's t-test. Relevant

primers were designed according to qPrimerDB (https://biodb.swu.edu.cn/qprimerdb) (Lu et al., 2018).

Yeast assays

For yeast two-hybrid assay, the CDS of *ONAC127* and *ONAC129* were cloned into the pGBKT7 and pGADT7 vector (Clontech). The fusion plasmids were transformed into yeast strain AH109 or Y187. The pGBKT7-53 was co-transformed with pGADT7-T as a positive control. For yeast one-hybrid assay, DNA fragments about 1000bp corresponding to the promoters of target genes were independently inserted into the pHisi-1 plasmid (Clontech). *ONAC127* and *ONAC129* were fused to GAL4 transcriptional activation domain (pGAD424). These constructs were transformed into the yeast strain YM4271. Yeast two-hybrid assay and one-hybrid assay were performed following the manufacturer's instructions (Clontech).

Chromatin immunoprecipitation (ChIP)

Overexpression lines of *ONAC127* and *ONAC129* (fused with 3×FLAG) were used for ChIP-Seq analyses. We verified the expression of target proteins by western blot using ANTI-FLAG M2 Monoclonal Antibody (Sigma-Aldrich). ChIP assay was performed with ANTI-FLAG M2 Magnetic Beads (Sigma-Aldrich) as the method described previously (Xiong et al., 2019). For each library, three independent replicated samples were prepared. The immunoprecipitated DNA and input DNA were subjected to being sequenced on the HiSeq 2000 platform (Illumina), which was processed by the Novogene Corporation.

ChIP-Seq raw sequencing data was mapped to the rice reference genome (RGAP ver. 7.0, http://rice.plantbiology.msu.edu) (Kawahara et al., 2013) using BWA (Li and Durbin, 2009). MACS2 (Zhang et al., 2008) was used for peak calling and the peaks were identified as significantly enriched (corrected P-value <0.05) in the IP libraries compared with input DNA. Visual analyses were performed using IGV (Intergative

Genomics Viewer, v2.3.26) (Robinson et al., 2011). Motif enrichment analyses were performed by MEME (Machanick and Bailey, 2011) with default parameters.

To validate the specific targets genes, the immunoprecipitated DNA and input DNA was applied for ChIP-qPCR analyses. The enrichment value was normalized to the input sample. The significance of differences was estimated using Student's t-test.

RNA-Seq

Total RNA was extracted from unripe caryopses at 7 DAP. For each library, three independent replicated RNA samples were prepared. The RNA samples were then sequenced on the HiSeq 2000 platform (Illumina), which was processed by the Novogene Corporation.

The raw reads were filtered for adaptors and low-quality reads. Clean reads were mapped to the reference genome of rice (RGAP v. 7.0) using HISAT2 (v.2.0.5) (Kim et al., 2015). The gene expression level was calculated by FPKM method (Trapnell et al., 2010), and the differentially expressed genes ($|\text{Fold Change}| \geq 2$ and p-value<0.05) were selected by DESeq2 software (Love et al., 2014). GOseq (Young et al., 2010) was used for GO enrichment analyses, and p-value was converted to $-\log_{10}(p\text{-value})$ for display.

***In vitro* GST pull-down assay**

The CDS of *ONAC127* and *ONAC129* were cloned into pET28a and pGEX-4-1 vectors respectively for His-tagged ONAC127 and GST-tagged ONAC129 protein expression *in vitro*. The fusion plasmids were transformed into *Escherichia coli* BL21 strain. The GST pull-down assays were performed according to the previous methods (Xiong et al., 2019). The protein was separated on a 10% SDS-PAGE gel and further analyzed by immunoblotting using anti-His and anti-GST antibody (Sigma-Aldrich).

581 **Dual Luciferase Transcriptional Activity Assay**

582 Full-length cDNAs of *ONAC127* and *ONAC129* were cloned to yeast GAL4
583 binding domain vectors (GAL4BD) and "None" as effectors. The 35S-GAL4-fLUC and
584 190-fLUC were used as reporters, and AtUbi::rLUC was used as an internal control.
585 The constructed plasmids were purified and transformed into rice protoplasts with the
586 procedure mentioned previously. Dual Luciferase Reporter Assay System (Promega)
587 was used to measure the luciferase activity by Tecan Infinite M200 (Tecan).

588 **Agronomic traits analyses**

589 Harvested ripe rice grains were air dried and stored at room temperature for at least
590 2 months before measuring. Only full grains were used for measuring 1000-grain
591 weight which was calculated based on 100 grains. The seed set rate/composition was
592 calculated based on the grains from 3-5 panicles (include the full, shrunken and blighted
593 grains). All measurements of the positive transgenic plants were undertaken using three
594 independent lines.
595

596 **Accession numbers**

597 The sequence data from this paper can be found in the RGAP database
598 (http://rice.plantbiology.msu.edu) under the following accession numbers: *ONAC025*
599 (LOC_Os11g31330), *ONAC127* (LOC_Os11g31340), *ONAC128* (LOC_Os11g31360),
600 *ONAC129* (LOC_Os11g31380), *OsMST6* (LOC_Os07g37320), *OsSWEET4*
601 (LOC_Os02g19820), *OsEATB* (LOC_Os09g28440), *OsMSR2* (LOC_Os01g72530),
602 *bHLH144* (LOC_Os04g35010), *OsHCI1* (LOC_Os10g30850), *HSP101*
603 (LOC_Os05g44340), *OsSWEET11* (LOC_Os08g42350), *OsSWEET15*
604 (LOC_Os02g30910), *OsbZIP63* (LOC_Os07g48820). The RNA-seq and ChIP-seq
605 data are deposited in the NCBI Gene Expression Omnibus (Edgar et al., 2002) with
606 accession number GSE140167.

607

608 **Supplemental Material**

609 **Supplemental Fig. S1** Expression level of mechanical isolation marker in isolated
610 tissue.
611 **Supplemental Fig. S2** Subcellular localization of the ONAC127 and ONAC129 in the
612 roots of two-week-old rice seedlings of pUbi::ONAC127-GFP and pUbi::ONAC129-
613 GFP transgenic plants.
614 **Supplemental Fig. S3** Mutation sites in *onac127*, *onac129* and *onac127;129* lines, as
615 compared with wild-type (ZH11) sequences.
616 **Supplemental Fig. S4** The relative expression level of the overexpression lines of
617 *ONAC127* and *ONAC129*.
618 **Supplemental Fig. S5** Different stages of caryopses development.
619 **Supplemental Fig. S6** Expression level of *ONAC127* and *ONAC129* in 7 DAP
620 caryopses of transgenic lines compared with that of ZH11.
621 **Supplemental Fig. S7** Detection of FLAG fusion proteins in the ZH11 and
622 overexpression lines.
623 **Supplemental Fig. S8** Expression level of the target genes of ONAC127 and
624 ONAC129 in 7 DAP caryopses of transgenic lines compared with that of ZH11.
625 **Supplemental Fig. S9** Expression level of the indirect target genes of ONAC127 and
626 ONAC129 in 7 DAP caryopses of transgenic lines compared with that of ZH11.
627 **Supplemental Table S1** Primers used in this study.
628 **Supplemental Dataset S1** Differentially expressed genes.
629 **Supplemental Dataset S2** Binding sites identified by ChIP-seq.
630

631 **ACKNOWLEDGEMENTS**

632 We thank Prof. Min Chen, Prof. Honghong Hu, Prof. Yidan Ouyang and Ms.

633 Wenjing Guo for helping revise the manuscript. This research was supported by grants
634 from the National Natural Science Foundation of China (no. 31570321). The funders
635 had no role in the study design, data collection and analysis, the decision to publish, or
636 in the preparation of the manuscript.
637

638 Author contributions

639 Y.R. and J.Y. conceived the original research plans; Y.R. carried out most of the
640 experiments; Z.H., Z.W., F.W. and Y.X. provided technical assistance to Y.R.; Y.R. and
641 H.J. analyzed the data; Y.R. conceived the project and wrote the article with
642 contributions of all the authors; J.Y. supervised and complemented the writing.
643

644 FIGURE

645 **Fig. 1 Spatial and temporal expression patterns of *ONAC127* and *ONAC129*.**
646 A. qRT-PCR analyses of *ONAC127* and *ONAC129* in different tissue. AL, aleurone
647 layer; Pe, pericarp; SE, starchy endosperm; Em, embryo; 1-21D, caryopses collected
648 during 1-21 DAP. The values in each column are the mean of three technical replicates
649 and the error bars indicate the ±SD. Ubiquitin is used as the reference gene. B. *In situ*
650 hybridization of sectioned caryopses collected at 1, 3, 5, 7 and 10 DAP using anti-sense
651 and sense probes. Nu, nucellar; Pe, pericarp; SE, starchy endosperm; Em, embryo; AL,
652 aleurone layer. Scale bars are 50 μm. C. Histochemical GUS activity detection using
653 pONAC127::GUS and pONAC129::GUS. Pe, pericarp; SE, starchy endosperm; Em,
654 embryo. Scale bar is 1 mm. D. Subcellular localization of the *ONAC127* and *ONAC129*
655 in rice protoplasts. 35S::Ghd7-CFP is used as a nuclear marker. Scale bars are 5 μm.
656

657 **Fig. 2 Interaction between ONAC127 & ONAC129.**
658 A. The yeast two-hybrid assay. The full-length cDNA of ONAC127 and ONAC129 are

659 both cloned into pGBKT7 (BD) and pGADT7 (AD). The transformants are grown on
660 [SD/–Trp /–Leu] and [SD/–Trp/–Leu/–His/–Ade] plates with 10^{0}, 10^{-1} and 10^{-2} fold
661 dilution. B. The pull-down assays showing that there is a direct interaction between
662 ONAC127-His and ONAC129-GST and *in vitro*. C. The BiFC assays of ONAC127 and
663 ONAC129. ONAC127-YFP^{N} and ONAC129-YFP^{C} interact to form a functional YFP
664 in rice protoplasts. 35S::Ghd7-CFP is used as a nuclear marker. Scale bars are 5 μm.
665
666 **Fig. 3 The construction of the CRISPR mutants and overexpression plants and**
667 **their phenotypes.**
668 A. Schematic diagram of the sgRNA target site in genomic region of *ONAC127* and
669 *ONAC129*. The target sequences of *onac127*, *onac129* and *onac127;129* are listed
670 under the diagram and marked as a colorful triangle. The Cas9 splice sites are marked
671 as red triangle and the protospacer-adjacent motifs are shown in orange. B. Schematic
672 diagram of the construction of OX127 & OX129. C. Phenotypes of grains of the
673 overexpression lines and mutants of *ONAC127* and *ONAC129*. Scale bars are 2 mm.
674 D. Phenotypes of panicles at maturation stage. The panicles of transgenic plants are
675 almost upright while the panicles of ZH11 are bent due to the grain filling. Scale bars
676 are 20 cm. E. Accumulation of starch in the pericarp of the caryopsis of
677 overexpression lines and mutants relative to ZH11. Cross sections of caryopses
678 stained with toluidine blue at 7DAP. Pe, pericarp; SE, starchy endosperm. Scale bar is
679 40 μm.
680
681 **Fig. 4 Agronomic traits analyses and ambient temperature.**
682 A. Seed set rate. The ratio of full grains to all spikelets on a panicle. B. 1,000 grains
683 weight. Only the fully filled grains were counted and the data was calculated based on
684 100 grains. C. The composition of the seed set of spikelets. Data in (A), (B) and (C)
685 are meant (±SD) from three independent lines, each of which are meant from three
686 biological replicates. Significant differences between the ZH11 and the transgenic

687 lines were determined using Student's t-test (* P<0.05, ** P<0.01). D and E. The
688 ambient temperature of growing areas during rice caryopsis filling stage. 35℃ is
689 marked as yellow dotted lines and 40℃ is marked as red dotted lines. T_S, heat damage
690 accumulated temperature during whole filling stage; H_S, heat damage hours during
691 whole filling stage; T_{S7}, heat damage accumulated temperature during 0-7 DAP; H_{S7},
692 heat damage hours during 0-7 DAP.
693
694 **Fig. 5 ONAC129 negatively regulates ONAC127 transcriptional activity.**
695 A. Scheme of the constructs used in the rice protoplast cotransfection assay. B. Data
696 of Dual-LUC assay. The reporter and internal control are co-transformed with each
697 experimental group. The fLUC/rLUC ratio represents the relative activity of
698 CaMV35S promoter. The values in each column are the mean (±SD) of three
699 replicates. Significant differences are determined using Student's t-test (** P<0.01).
700 C. Schematic diagram of the domains of ONAC127 & ONAC129. The color legends
701 indicating the domains are shown at the bottom of the figure.
702
703 **Fig. 6 Data analyses of RNA-Seq and ChIP-Seq.**
704 A and B. Venn diagram showing the number of genes regulated by *ONAC127* and
705 *ONAC129* based on the RNA-seq analyses. Differentially expressed genes are defined
706 as |Fold Change|≥2 and *p*-value<0.05. *p*-values were calculated using the Fisher's
707 exact test. C. A selection of enriched gene ontology (GO) terms of the differentially
708 expressed genes. GO terms with FDR <0.05 were kept. The length of the bars
709 represents the negative logarithm (base 10) of FDR. D. Venn diagram showing the
710 number of ONAC127 and ONAC129 direct target genes. The red trapezoid indicates
711 the ONAC127 and ONAC129 preferable bound genes. E and F. Motif analyses of
712 ONAC127 and ONAC129 binding peaks. The E-value is the enrichment P-value
713 multiplied by the number of candidate motifs tested.
714

Fig. 7 Identification and validation of ONAC127 and ONAC129 direct target genes in rice.

A. The interaction between ONAC127/129 and the promoters of PTGs as determined by yeast one-hybrid analyses. The transformants were grown on [SD/–Leu /–His] plates with 3-AT which concentrations were 50mM, 100mM and 150mM respectively. B. Scheme of the constructs used in the rice protoplast cotransfection assay. C. Data of Dual-LUC assay. The fLUC/rLUC ratio represents the relative activity of target gene promoters. D-G. ChIP-qPCR verification of ONAC127 and ONAC129 binding regions. The values in each column are the mean (±SD) of three replicates. Significant differences were determined using Student's t-test (* $P<0.05$; ** $P<0.01$).

Fig. 8 Schematic diagram of the working model of ONAC127 and ONAC129 in rice caryopsis.

ONAC127 and ONAC129 regulate the expression of *OsMST6* and *OsSWEET4* directly to participate in the apoplasmic transportation, and OsSWEET11 and OsSWEET15 may be also involved in this process as the indirect downstream transporters of them. When heat stress occurs, ONAC127 and ONAC129 may be involved in the response to heat stress during the filling stage by regulating the expression of *OsMSR2* and *OsEATB* directly, while *OsHCI1* and *OsHSP101* are regulated indirectly. ONAC127 and ONAC129 may act as the balancer of apoplasmic transportation and the core transcription factors in the stress response during the early and middle stages of rice caryopsis development.

LITERATURE CITED

Agarwal P, Kapoor S, Tyagi AK (2011) Transcription factors regulating the progression of monocot and dicot seed development. Bioessays **33:** 189-202

Bai AN, Lu XD, Li DQ, Liu JX, Liu CM (2016) NF-YB1-regulated expression of sucrose transporters in aleurone facilitates sugar loading to rice endosperm. Cell Res **26:** 384-388

Chen S, Zhang T, Huang Q, Chen M, Zhao L, Zhang Y (2019) Effects of High Temperature Injury

744 on Seed Setting Rate from Heading to Milky Stage of Early Season Rice in Hainan. China
745 Tropical Agriculture**:** 65-69 (in Chinese with English abstract)
746 **Chen X, Lu S, Wang Y, Zhang X, Lv B, Luo L, Xi D, Shen J, Ma H, Ming F** (2015) OsNAC2 encoding
747 a NAC transcription factor that affects plant height through mediating the gibberellic acid
748 pathway in rice. Plant J **82:** 302-314
749 **Christianson JA, Dennis ES, Llewellyn DJ, Wilson IW** (2010) ATAF NAC transcription factors:
750 regulators of plant stress signaling. Plant Signal Behav **5:** 428-432
751 **Edgar R, Domrachev M, Lash AE** (2002) Gene Expression Omnibus: NCBI gene expression and
752 hybridization array data repository. Nucleic Acids Res **30:** 207-210
753 **Fang Y, Liao K, Du H, Xu Y, Song H, Li X, Xiong L** (2015) A stress-responsive NAC transcription
754 factor SNAC3 confers heat and drought tolerance through modulation of reactive oxygen
755 species in rice. J Exp Bot **66:** 6803-6817
756 **Fang Y, Xie K, Xiong L** (2014) Conserved miR164-targeted NAC genes negatively regulate
757 drought resistance in rice. J Exp Bot **65:** 2119-2135
758 **Fang Y, You J, Xie K, Xie W, Xiong L** (2008) Systematic sequence analysis and identification of
759 tissue-specific or stress-responsive genes of NAC transcription factor family in rice. Mol
760 Genet Genomics **280:** 547-563
761 **Fujita M, Fujita Y, Maruyama K, Seki M, Hiratsu K, Ohme-Takagi M, Tran LS, Yamaguchi-**
762 **Shinozaki K, Shinozaki K** (2004) A dehydration-induced NAC protein, RD26, is involved
763 in a novel ABA-dependent stress-signaling pathway. Plant J **39:** 863-876
764 **Hakata M, Wada H, Masumoto-Kubo C, Tanaka R, Sato H, Morita S** (2017) Development of a
765 new heat tolerance assay system for rice spikelet sterility. Plant Methods **13:** 34
766 **Hao YJ, Song QX, Chen HW, Zou HF, Wei W, Kang XS, Ma B, Zhang WK, Zhang JS, Chen SY**
767 (2010) Plant NAC-type transcription factor proteins contain a NARD domain for
768 repression of transcriptional activation. Planta **232:** 1033-1043
769 **Hoshikawa K** (1984) Development of Endosperm Tissue with Special Reference to the
770 Translocation of Reserve Substances in Cereals : III. Translocation pathways in rice
771 endosperm. Japanese journal of crop science **53:** 153-162
772 **Hu H, Dai M, Yao J, Xiao B, Li X, Zhang Q, Xiong L** (2006) Overexpressing a NAM, ATAF, and
773 CUC (NAC) transcription factor enhances drought resistance and salt tolerance in rice.
774 Proc Natl Acad Sci U S A **103:** 12987-12992
775 **Hu H, Xiong L** (2014) Genetic engineering and breeding of drought-resistant crops. Annu Rev
776 Plant Biol **65:** 715-741
777 **Huang D, Wang S, Zhang B, Shang-Guan K, Shi Y, Zhang D, Liu X, Wu K, Xu Z, Fu X, Zhou Y**
778 (2015) A Gibberellin-Mediated DELLA-NAC Signaling Cascade Regulates Cellulose
779 Synthesis in Rice. Plant Cell **27:** 1681-1696
780 **Ishimaru T, Ida M, Hirose S, Shimamura S, Masumura T, Nishizawa NK, Nakazono M, Kondo**
781 **M** (2015) Laser microdissection-based gene expression analysis in the aleurone layer and
782 starchy endosperm of developing rice caryopses in the early storage phase. Rice (N Y) **8:**
783 57
784 **Kawahara Y, de la Bastide M, Hamilton JP, Kanamori H, McCombie WR, Ouyang S, Schwartz**
785 **DC, Tanaka T, Wu J, Zhou S, Childs KL, Davidson RM, Lin H, Quesada-Ocampo L,**

Vaillancourt B, Sakai H, Lee SS, Kim J, Numa H, Itoh T, Buell CR, Matsumoto T (2013) Improvement of the Oryza sativa Nipponbare reference genome using next generation sequence and optical map data. Rice (N Y) **6:** 4

Kim D, Langmead B, Salzberg SL (2015) HISAT: a fast spliced aligner with low memory requirements. Nat Methods **12:** 357-360

Koini MA, Alvey L, Allen T, Tilley CA, Harberd NP, Whitelam GC, Franklin KA (2009) High temperature-mediated adaptations in plant architecture require the bHLH transcription factor PIF4. Curr Biol **19:** 408-413

Kouchi H, Hata S (1993) Isolation and characterization of novel nodulin cDNAs representing genes expressed at early stages of soybean nodule development. Mol Gen Genet **238:** 106-119

Li B, Gao K, Ren H, Tang W (2018) Molecular mechanisms governing plant responses to high temperatures. J Integr Plant Biol **60:** 757-779

Li H, Durbin R (2009) Fast and accurate short read alignment with Burrows-Wheeler transform. Bioinformatics **25:** 1754-1760

Lim SD, Cho HY, Park YC, Ham DJ, Lee JK, Jang CS (2013) The rice RING finger E3 ligase, OsHCI1, drives nuclear export of multiple substrate proteins and its heterogeneous overexpression enhances acquired thermotolerance. J Exp Bot **64:** 2899-2914

Lin MY, Chai KH, Ko SS, Kuang LY, Lur HS, Charng YY (2014) A positive feedback loop between HEAT SHOCK PROTEIN101 and HEAT STRESS-ASSOCIATED 32-KD PROTEIN modulates long-term acquired thermotolerance illustrating diverse heat stress responses in rice varieties. Plant Physiol **164:** 2045-2053

Lin YJ, Zhang Q (2005) Optimising the tissue culture conditions for high efficiency transformation of indica rice. Plant Cell Rep **23:** 540-547

Lindemose S, Jensen MK, Van de Velde J, O'Shea C, Heyndrickx KS, Workman CT, Vandepoele K, Skriver K, De Masi F (2014) A DNA-binding-site landscape and regulatory network analysis for NAC transcription factors in Arabidopsis thaliana. Nucleic Acids Res **42:** 7681-7693

Liu H, Ding Y, Zhou Y, Jin W, Xie K, Chen LL (2017) CRISPR-P 2.0: An Improved CRISPR-Cas9 Tool for Genome Editing in Plants. Mol Plant **10:** 530-532

Liu HT, Li B, Shang ZL, Li XZ, Mu RL, Sun DY, Zhou RG (2003) Calmodulin is involved in heat shock signal transduction in wheat. Plant Physiol **132:** 1186-1195

Liu W, Xie X, Ma X, Li J, Chen J, Liu YG (2015) DSDecode: A Web-Based Tool for Decoding of Sequencing Chromatograms for Genotyping of Targeted Mutations. Mol Plant **8:** 1431-1433

Livak KJ, Schmittgen TD (2001) Analysis of relative gene expression data using real-time quantitative PCR and the 2(-Delta Delta C(T)) Method. Methods **25:** 402-408

Love MI, Huber W, Anders S (2014) Moderated estimation of fold change and dispersion for RNA-seq data with DESeq2. Genome Biology **15**

Lu K, Li T, He J, Chang W, Zhang R, Liu M, Yu M, Fan Y, Ma J, Sun W, Qu C, Liu L, Li N, Liang Y, Wang R, Qian W, Tang Z, Xu X, Lei B, Zhang K, Li J (2018) qPrimerDB: a thermodynamics-based gene-specific qPCR primer database for 147 organisms. Nucleic Acids Res **46:** D1229-D1236

Ma X, Zhang Q, Zhu Q, Liu W, Chen Y, Qiu R, Wang B, Yang Z, Li H, Lin Y, Xie Y, Shen R, Chen S, Wang Z, Chen Y, Guo J, Chen L, Zhao X, Dong Z, Liu YG (2015) A Robust CRISPR/Cas9 System for Convenient, High-Efficiency Multiplex Genome Editing in Monocot and Dicot Plants. Mol Plant **8:** 1274-1284

Machanick P, Bailey TL (2011) MEME-ChIP: motif analysis of large DNA datasets. Bioinformatics **27:** 1696-1697

Mao C, Ding W, Wu Y, Yu J, He X, Shou H, Wu P (2007) Overexpression of a NAC-domain protein promotes shoot branching in rice. New Phytol **176:** 288-298

Mathew IE, Das S, Mahto A, Agarwal P (2016) Three Rice NAC Transcription Factors Heteromerize and Are Associated with Seed Size. Front Plant Sci **7:** 1638

Matsuda T, Kawahara H, Chonan N (1979) Histo-Cytological Researches on Translocation and Ripening in Rice Ovary : I. Histological changes and transfer pathways in the developing ovary. Japanese journal of crop science **48:** 155-162

Nuruzzaman M, Manimekalai R, Sharoni AM, Satoh K, Kondoh H, Ooka H, Kikuchi S (2010) Genome-wide analysis of NAC transcription factor family in rice. Gene **465:** 30-44

Olsen AN, Ernst HA, Leggio LL, Skriver K (2005) DNA-binding specificity and molecular functions of NAC transcription factors. Plant Science **169:** 785-797

Ooka H, Satoh K, Doi K, Nagata T, Otomo Y, Murakami K, Matsubara K, Osato N, Kawai J, Carninci P, Hayashizaki Y, Suzuki K, Kojima K, Takahara Y, Yamamoto K, Kikuchi S (2003) Comprehensive analysis of NAC family genes in Oryza sativa and Arabidopsis thaliana. DNA Res **10:** 239-247

Oono Y, Wakasa Y, Hirose S, Yang L, Sakuta C, Takaiwa F (2010) Analysis of ER stress in developing rice endosperm accumulating beta-amyloid peptide. Plant Biotechnol J **8:** 691-718

Oparka KJ, Gates P (1981) Transport of assimilates in the developing caryopsis of rice (Oryza sativa L.) : The pathways of water and assimilated carbon. Planta **152:** 388-396

Patrick JW (1997) PHLOEM UNLOADING: Sieve Element Unloading and Post-Sieve Element Transport. Annu Rev Plant Physiol Plant Mol Biol **48:** 191-222

Qi W, Sun F, Wang Q, Chen M, Huang Y, Feng YQ, Luo X, Yang J (2011) Rice ethylene-response AP2/ERF factor OsEATB restricts internode elongation by down-regulating a gibberellin biosynthetic gene. Plant Physiol **157:** 216-228

Robinson JT, Thorvaldsdottir H, Winckler W, Guttman M, Lander ES, Getz G, Mesirov JP (2011) Integrative genomics viewer. Nat Biotechnol **29:** 24-26

Schramm F, Larkindale J, Kiehlmann E, Ganguli A, Englich G, Vierling E, von Koskull-Doring P (2008) A cascade of transcription factor DREB2A and heat stress transcription factor HsfA3 regulates the heat stress response of Arabidopsis. Plant J **53:** 264-274

Shen J, Liu J, Xie K, Xing F, Xiong F, Xiao J, Li X, Xiong L (2017) Translational repression by a miniature inverted-repeat transposable element in the 3' untranslated region. Nat Commun **8:** 14651

Shen J, Lv B, Luo L, He J, Mao C, Xi D, Ming F (2017) The NAC-type transcription factor OsNAC2 regulates ABA-dependent genes and abiotic stress tolerance in rice. Sci Rep **7:** 40641

Singh A, Mittal D, Lavania D, Agarwal M, Mishra RC, Grover A (2012) OsHsfA2c and OsHsfB4b

are involved in the transcriptional regulation of cytoplasmic OsClpB (Hsp100) gene in rice (Oryza sativa L.). Cell Stress Chaperones **17:** 243-254

Sosso D, Luo D, Li QB, Sasse J, Yang J, Gendrot G, Suzuki M, Koch KE, McCarty DR, Chourey PS, Rogowsky PM, Ross-Ibarra J, Yang B, Frommer WB (2015) Seed filling in domesticated maize and rice depends on SWEET-mediated hexose transport. Nat Genet **47:** 1489-1493

Trapnell C, Williams BA, Pertea G, Mortazavi A, Kwan G, van Baren MJ, Salzberg SL, Wold BJ, Pachter L (2010) Transcript assembly and quantification by RNA-Seq reveals unannotated transcripts and isoform switching during cell differentiation. Nat Biotechnol **28:** 511-515

Waadt R, Schmidt LK, Lohse M, Hashimoto K, Bock R, Kudla J (2008) Multicolor bimolecular fluorescence complementation reveals simultaneous formation of alternative CBL/CIPK complexes in planta. Plant J **56:** 505-516

Walter M, Chaban C, Schutze K, Batistic O, Weckermann K, Nake C, Blazevic D, Grefen C, Schumacher K, Oecking C, Harter K, Kudla J (2004) Visualization of protein interactions in living plant cells using bimolecular fluorescence complementation. Plant J **40:** 428-438

Wang L, Xie W, Chen Y, Tang W, Yang J, Ye R, Liu L, Lin Y, Xu C, Xiao J, Zhang Q (2010) A dynamic gene expression atlas covering the entire life cycle of rice. Plant J **61:** 752-766

Wang L, Zhou Z, Song X, Li J, Deng X, Mei F (2008) Evidence of ceased programmed cell death in metaphloem sieve elements in the developing caryopsis of Triticum aestivum L. Protoplasma **234:** 87-96

Wang Y, Xiao Y, Zhang Y, Chai C, Wei G, Wei X, Xu H, Wang M, Ouwerkerk PB, Zhu Z (2008) Molecular cloning, functional characterization and expression analysis of a novel monosaccharide transporter gene OsMST6 from rice (Oryza sativa L.). Planta **228:** 525-535

Wu X, Liu J, Li D, Liu CM (2016) Rice caryopsis development II: Dynamic changes in the endosperm. J Integr Plant Biol **58:** 786-798

Xiong Y, Ren Y, Li W, Wu F, Yang W, Huang X, Yao J (2019) NF-YC12 is a key multi-functional regulator of accumulation of seed storage substances in rice. J Exp Bot **70:** 3765-3780

Xu GY, Rocha PS, Wang ML, Xu ML, Cui YC, Li LY, Zhu YX, Xia X (2011) A novel rice calmodulin-like gene, OsMSR2, enhances drought and salt tolerance and increases ABA sensitivity in Arabidopsis. Planta **234:** 47-59

Xue W, Xing Y, Weng X, Zhao Y, Tang W, Wang L, Zhou H, Yu S, Xu C, Li X, Zhang Q (2008) Natural variation in Ghd7 is an important regulator of heading date and yield potential in rice. Nat Genet **40:** 761-767

Yamaguchi M, Ohtani M, Mitsuda N, Kubo M, Ohme-Takagi M, Fukuda H, Demura T (2010) VND-INTERACTING2, a NAC domain transcription factor, negatively regulates xylem vessel formation in Arabidopsis. Plant Cell **22:** 1249-1263

Yang J, Luo D, Yang B, Frommer WB, Eom JS (2018) SWEET11 and 15 as key players in seed filling in rice. New Phytol

Yang SD, Seo PJ, Yoon HK, Park CM (2011) The Arabidopsis NAC transcription factor VNI2 integrates abscisic acid signals into leaf senescence via the COR/RD genes. Plant Cell **23:** 2155-2168

912 **Young MD, Wakefield MJ, Smyth GK, Oshlack A** (2010) Gene ontology analysis for RNA-seq:
913 accounting for selection bias. Genome Biol **11:** R14
914 **Zhang WH, Zhou YC, Dibley KE, Tyerman SD, Furbank RT, Patrick JW** (2007) Nutrient loading
915 of developing seeds. Functional Plant Biology **34:** 314-331
916 **Zhang Y, Liu T, Meyer CA, Eeckhoute J, Johnson DS, Bernstein BE, Nusbaum C, Myers RM,**
917 **Brown M, Li W, Liu XS** (2008) Model-based analysis of ChIP-Seq (MACS). Genome Biol
918 **9:** R137
919 **Zhang Z, Dong J, Ji C, Wu Y, Messing J** (2019) NAC-type transcription factors regulate
920 accumulation of starch and protein in maize seeds. Proc Natl Acad Sci U S A **116:** 11223-
921 11228

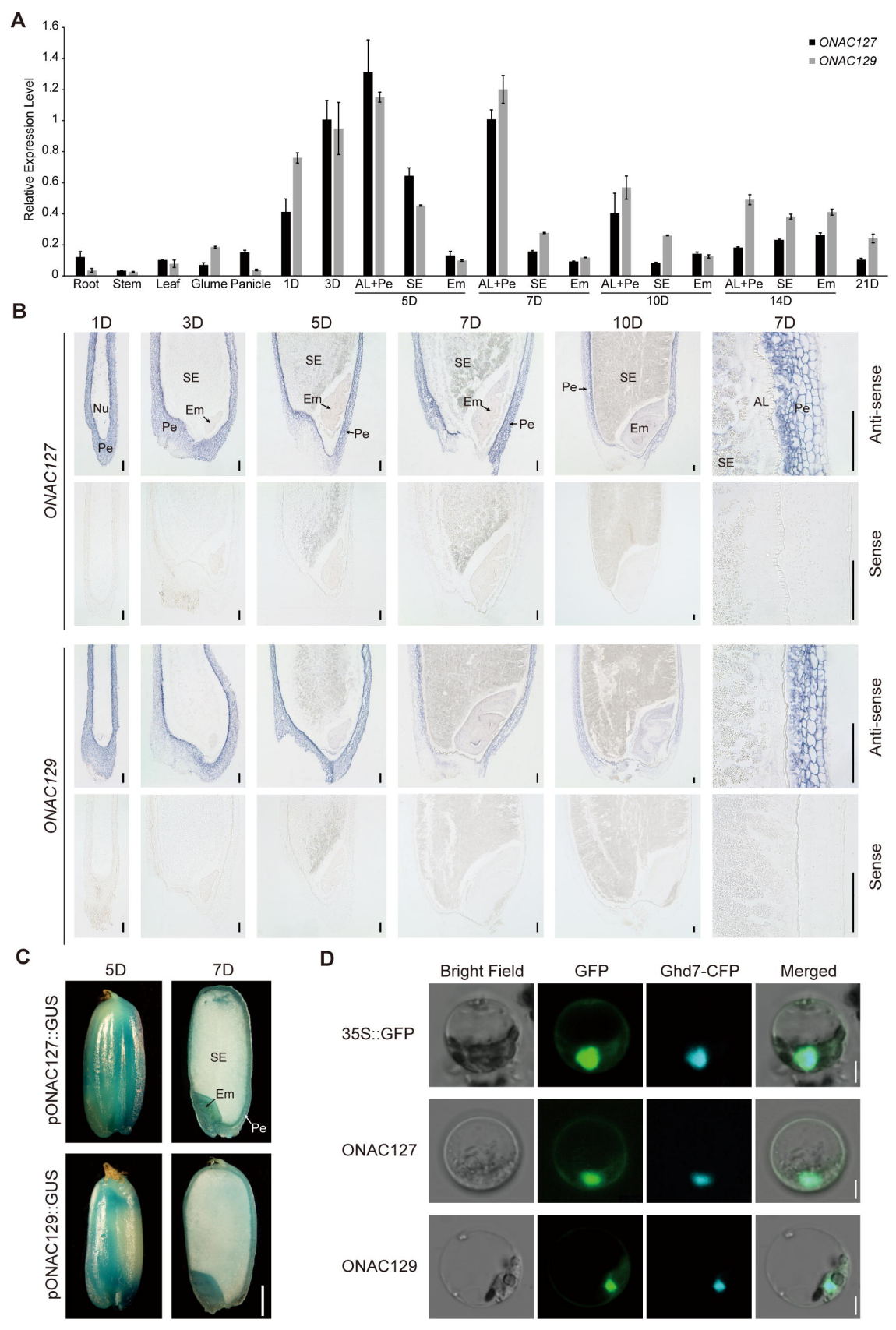
A
Relative Expression Level
ONAC127
ONAC129
Root
Stem
Leaf
Glume
Panicle
1D
3D
AL+Pe
SE
Em
5D
7D
10D
14D
21D
B
1D
3D
5D
7D
10D
7D
ONAC127
ONAC129
Anti-sense
Sense
Nu
Pe
SE
Em
AL
C
5D
7D
pONAC127::GUS
pONAC129::GUS
D
Bright Field
GFP
Ghd7-CFP
Merged
35S::GFP
ONAC127
ONAC129

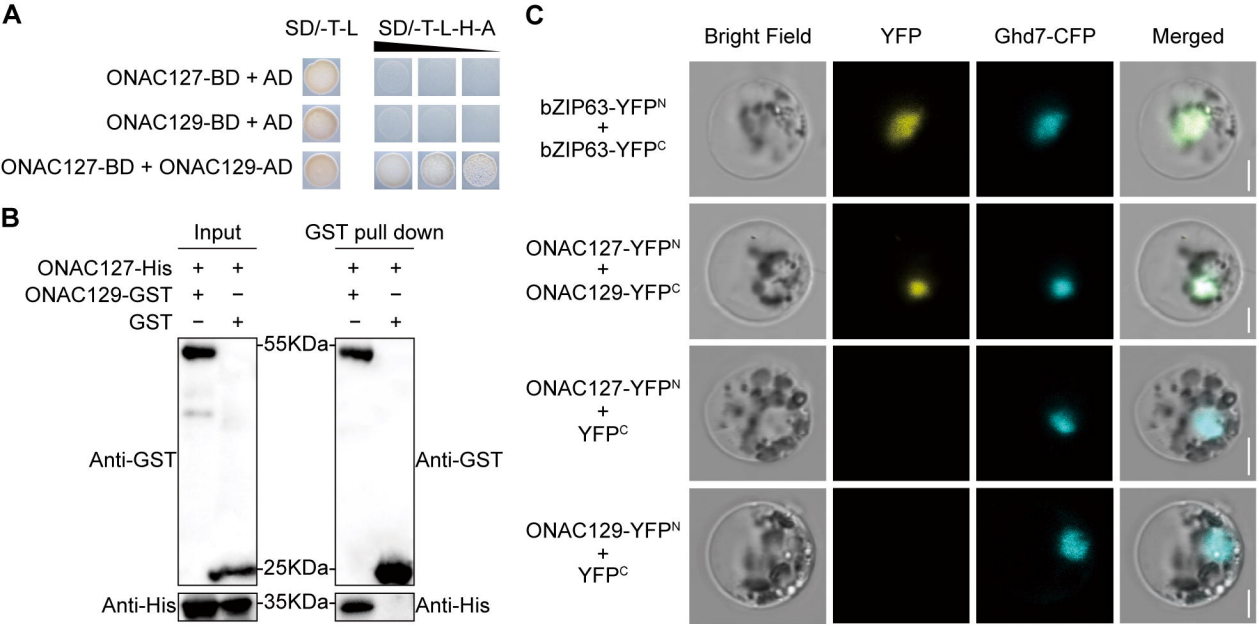
A
SD/-T-L
SD/-T-L-H-A
ONAC127-BD + AD
ONAC129-BD + AD
ONAC127-BD + ONAC129-AD
B
Input
GST pull down
ONAC127-His + + + +
ONAC129-GST + − + −
GST − + − +
55KDa
25KDa
35KDa
Anti-GST
Anti-GST
Anti-His
Anti-His
C
Bright Field
YFP
Ghd7-CFP
Merged
bZIP63-YFP^N + bZIP63-YFP^C
ONAC127-YFP^N + ONAC129-YFP^C
ONAC127-YFP^N + YFP^C
ONAC129-YFP^N + YFP^C

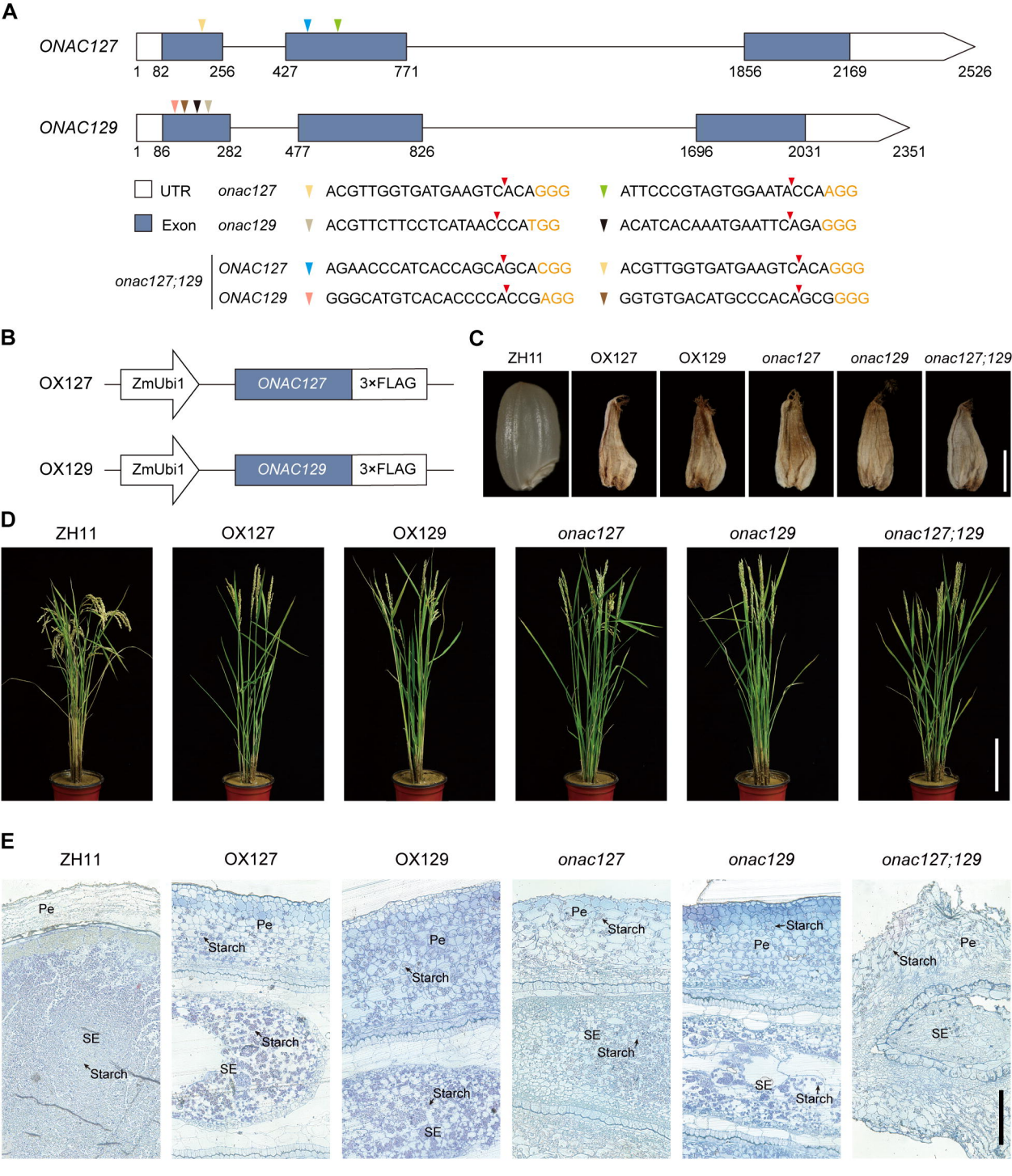
A
ONAC127
1 82 256 427 771 1856 2169 2526
ONAC129
1 86 282 477 826 1696 2031 2351
UTR
Exon
onac127 ACGTTGGTGATGAAGTCACAGGG ATTCCCGTAGTGGAATACCAAGG
onac129 ACGTTCTTCCTCATAACCCATGG ACATCACAAATGAATTCAGAGGG
onac127;129
ONAC127 AGAACCCATCACCAGCAGCACGG ACGTTGGTGATGAAGTCACAGGG
ONAC129 GGGCATGTCACACCCCACCGAGG GGTGTGACATGCCCACAGCGGGG
B
OX127
ZmUbi1
ONAC127
3×FLAG
OX129
ZmUbi1
ONAC129
3×FLAG
C
ZH11
OX127
OX129
onac127
onac129
onac127;129
D
ZH11
OX127
OX129
onac127
onac129
onac127;129
E
ZH11
OX127
OX129
onac127
onac129
onac127;129
Pe
SE
Starch

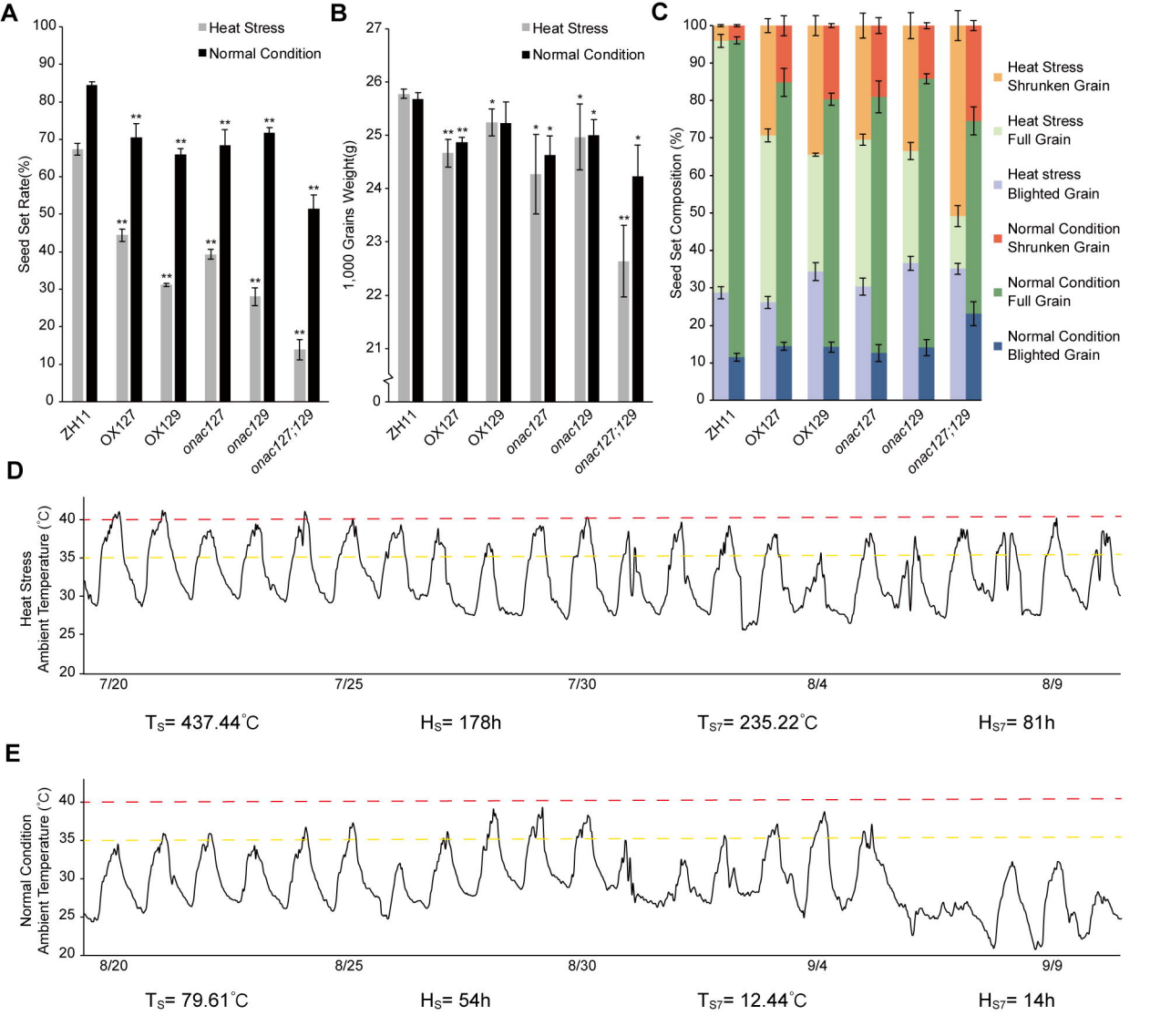
A
Heat Stress
Normal Condition
Seed Set Rate(%)
ZH11
OX127
OX129
onac127
onac129
onac127;129
B
Heat Stress
Normal Condition
1,000 Grains Weight(g)
C
Seed Set Composition (%)
Heat Stress Shrunken Grain
Heat Stress Full Grain
Heat stress Blighted Grain
Normal Condition Shrunken Grain
Normal Condition Full Grain
Normal Condition Blighted Grain
D
Heat Stress Ambient Temperature (˚C)
7/20
7/25
7/30
8/4
8/9
TS= 437.44˚C
HS= 178h
TS7= 235.22˚C
HS7= 81h
E
Normal Condition Ambient Temperature (˚C)
8/20
8/25
8/30
9/4
9/9
TS= 79.61˚C
HS= 54h
TS7= 12.44˚C
HS7= 14h

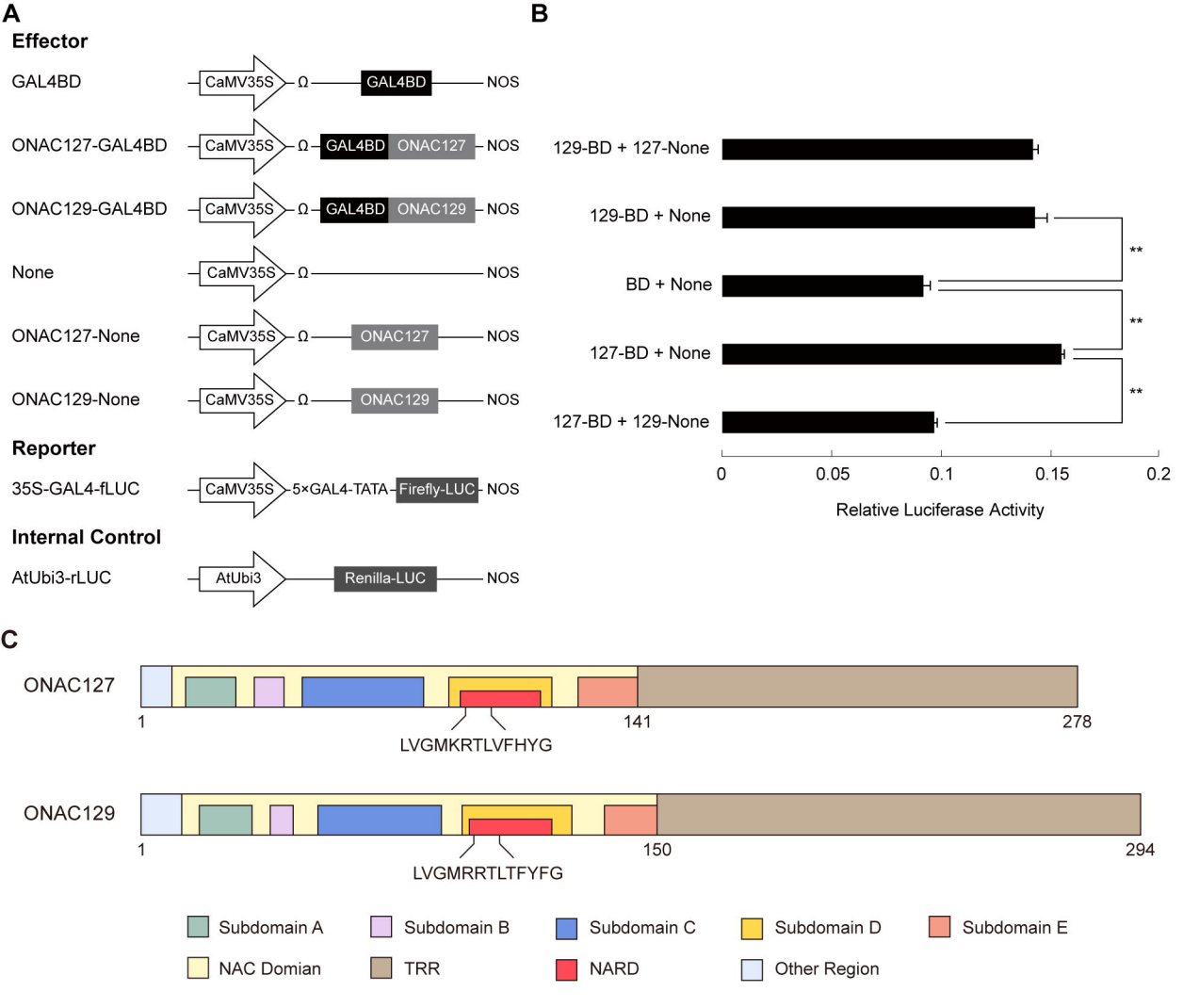
A
Effector
GAL4BD
CaMV35S
Ω
GAL4BD
NOS
ONAC127-GAL4BD
GAL4BD
ONAC127
ONAC129-GAL4BD
GAL4BD
ONAC129
None
ONAC127-None
ONAC127
ONAC129-None
ONAC129
Reporter
35S-GAL4-fLUC
5×GAL4-TATA
Firefly-LUC
Internal Control
AtUbi3-rLUC
AtUbi3
Renilla-LUC
B
129-BD + 127-None
129-BD + None
BD + None
127-BD + None
127-BD + 129-None
**
**
**
0
0.05
0.1
0.15
0.2
Relative Luciferase Activity
C
ONAC127
1
141
278
LVGMKRTLVFHYG
ONAC129
1
150
294
LVGMRRTLTFYFG
Subdomain A
Subdomain B
Subdomain C
Subdomain D
Subdomain E
NAC Domian
TRR
NARD
Other Region

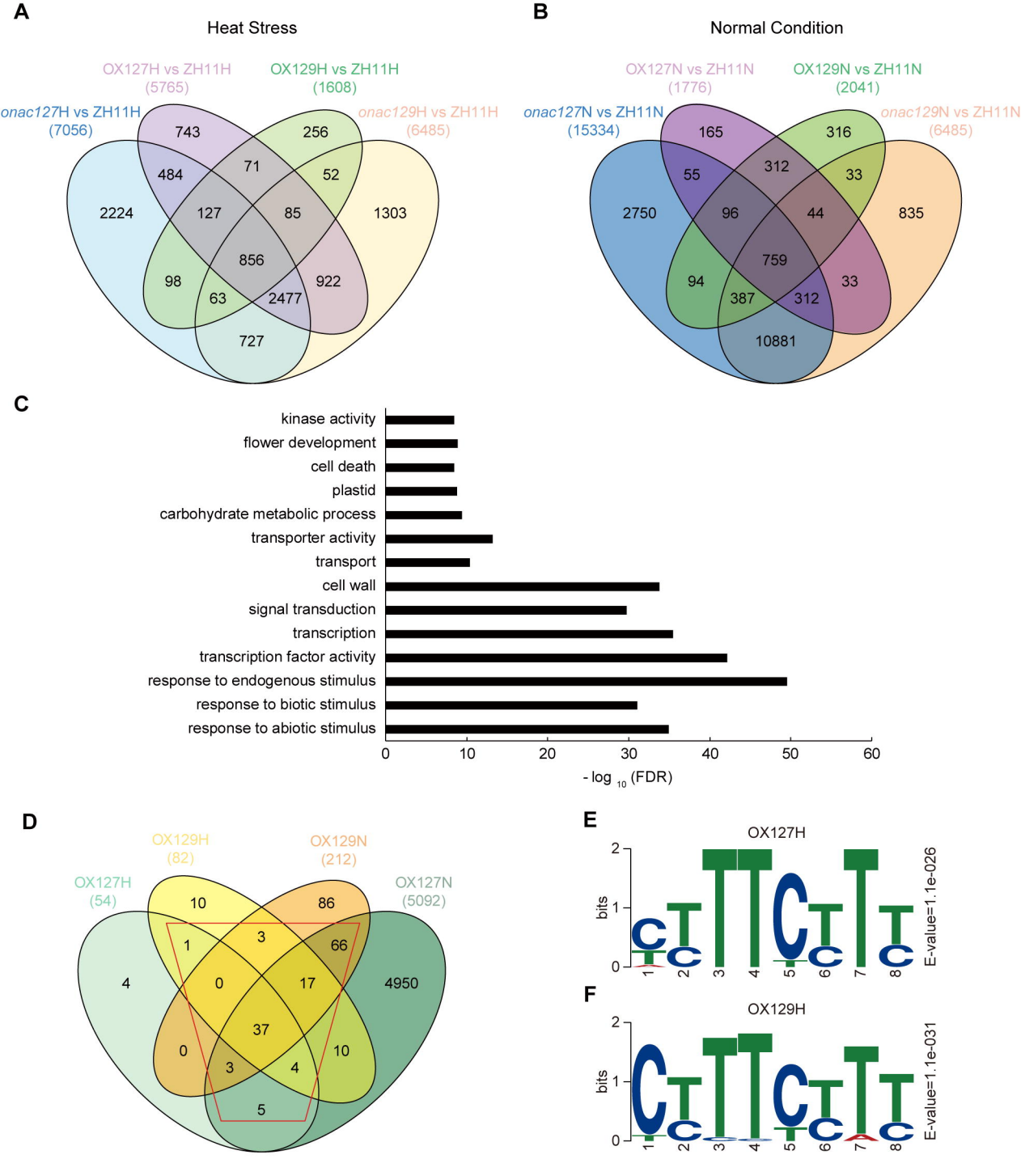
A
Heat Stress
OX127H vs ZH11H
(5765)
OX129H vs ZH11H
(1608)
onac127H vs ZH11H
(7056)
onac129H vs ZH11H
(6485)
743
256
484
71
52
2224
127
85
1303
856
98
922
63
2477
727
B
Normal Condition
OX127N vs ZH11N
(1776)
OX129N vs ZH11N
(2041)
onac127N vs ZH11N
(15334)
onac129N vs ZH11N
(6485)
165
316
312
55
33
2750
96
44
835
759
94
33
387
312
10881
C
kinase activity
flower development
cell death
plastid
carbohydrate metabolic process
transporter activity
transport
cell wall
signal transduction
transcription
transcription factor activity
response to endogenous stimulus
response to biotic stimulus
response to abiotic stimulus
0
10
20
30
40
50
60
- log 10 (FDR)
D
OX129H
(82)
OX129N
(212)
OX127H
(54)
OX127N
(5092)
10
86
1
3
66
4
0
17
4950
37
0
10
3
4
5
E
OX127H
bits
2
1
0
1
2
3
4
5
6
7
8
E-value=1.1e-026
F
OX129H
bits
2
1
0
1
2
3
4
5
6
7
8
E-value=1.1e-031

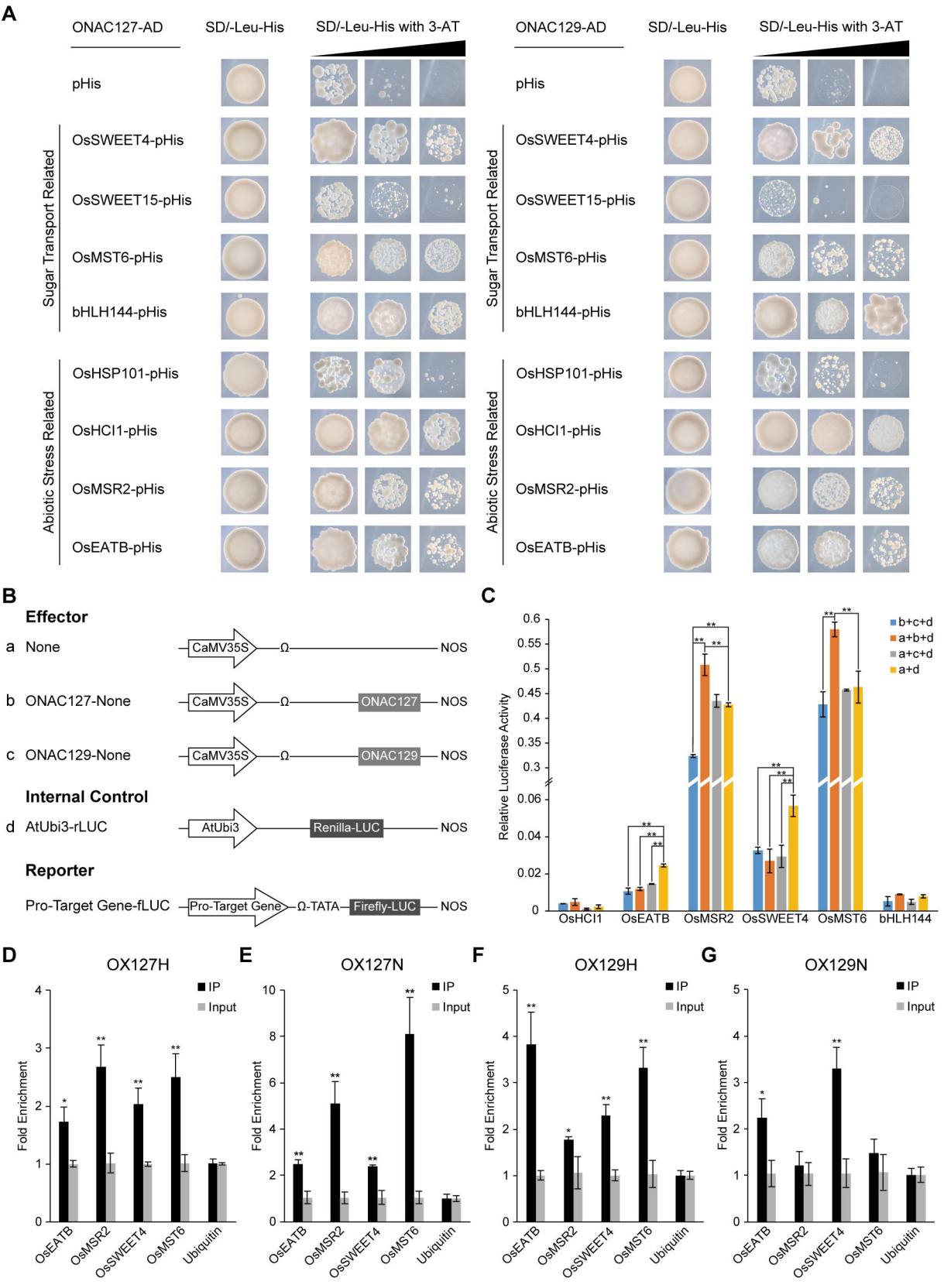
A
ONAC127-AD
SD/-Leu-His
SD/-Leu-His with 3-AT
ONAC129-AD
SD/-Leu-His
SD/-Leu-His with 3-AT
pHis
OsSWEET4-pHis
OsSWEET15-pHis
OsMST6-pHis
bHLH144-pHis
OsHSP101-pHis
OsHCI1-pHis
OsMSR2-pHis
OsEATB-pHis
Sugar Transport Related
Abiotic Stress Related
B
Effector
a None
CaMV35S
Ω
NOS
b ONAC127-None
ONAC127
c ONAC129-None
ONAC129
Internal Control
d AtUbi3-rLUC
AtUbi3
Renilla-LUC
Reporter
Pro-Target Gene-fLUC
Pro-Target Gene
Ω-TATA
Firefly-LUC
C
Relative Luciferase Activity
b+c+d
a+b+d
a+c+d
a+d
OsHCI1
OsEATB
OsMSR2
OsSWEET4
OsMST6
bHLH144
D
OX127H
E
OX127N
F
OX129H
G
OX129N
IP
Input
Fold Enrichment
OsEATB
OsMSR2
OsSWEET4
OsMST6
Ubiquitin

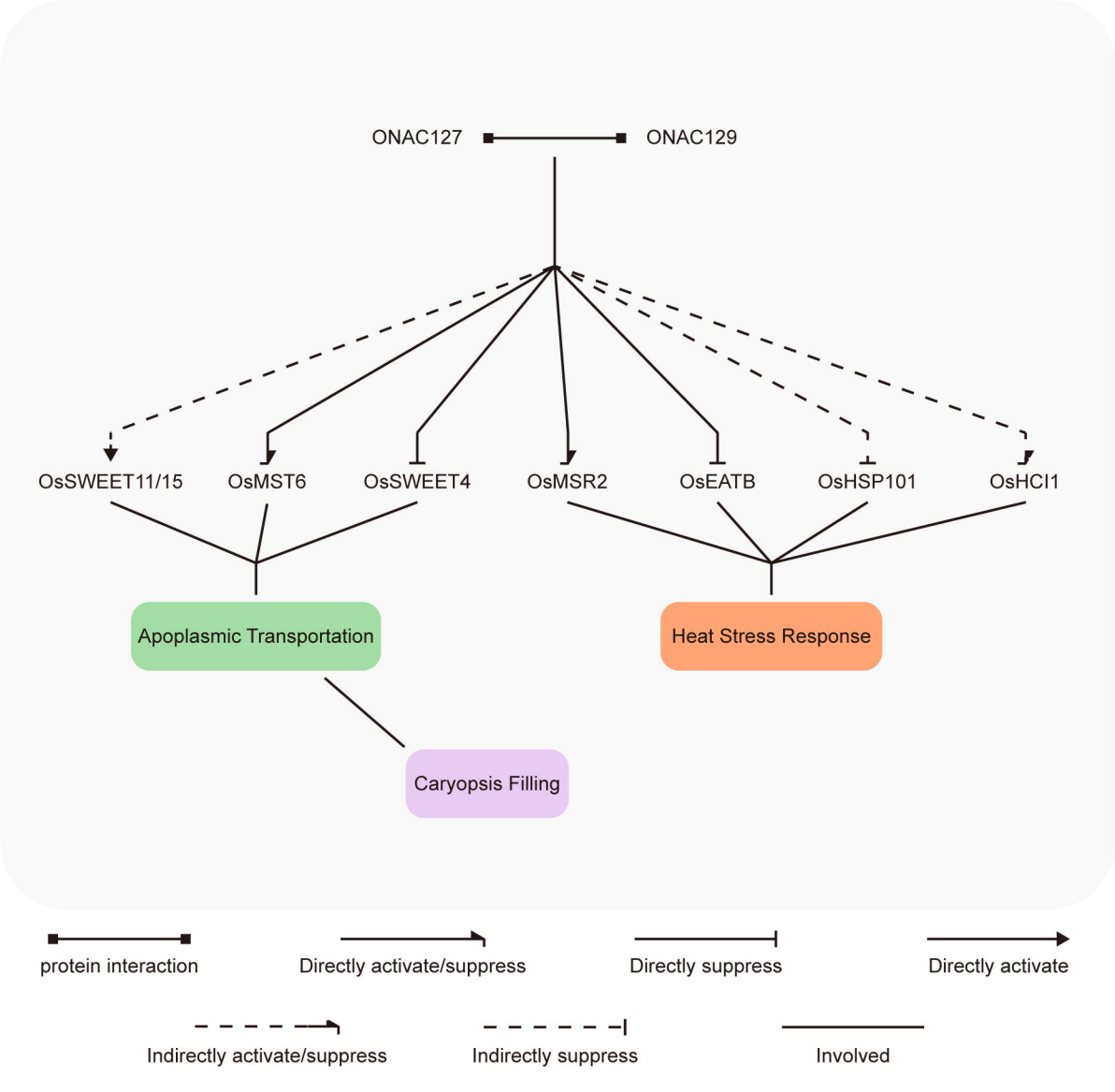
ONAC127
ONAC129
OsSWEET11/15
OsMST6
OsSWEET4
OsMSR2
OsEATB
OsHSP101
OsHCI1
Apoplasmic Transportation
Heat Stress Response
Caryopsis Filling
protein interaction
Directly activate/suppress
Directly suppress
Directly activate
Indirectly activate/suppress
Indirectly suppress
Involved